

Effective Field Theory Breakdown Near Cool Black Holes

Grant Remmen

Center for Cosmology and Particle Physics
New York University

2303.07358, 2403.00051
with G. Horowitz, M. Kolanowski, and J. Santos

Solvay Workshop on Near-Extremal Black Holes
Brussels
September 2024



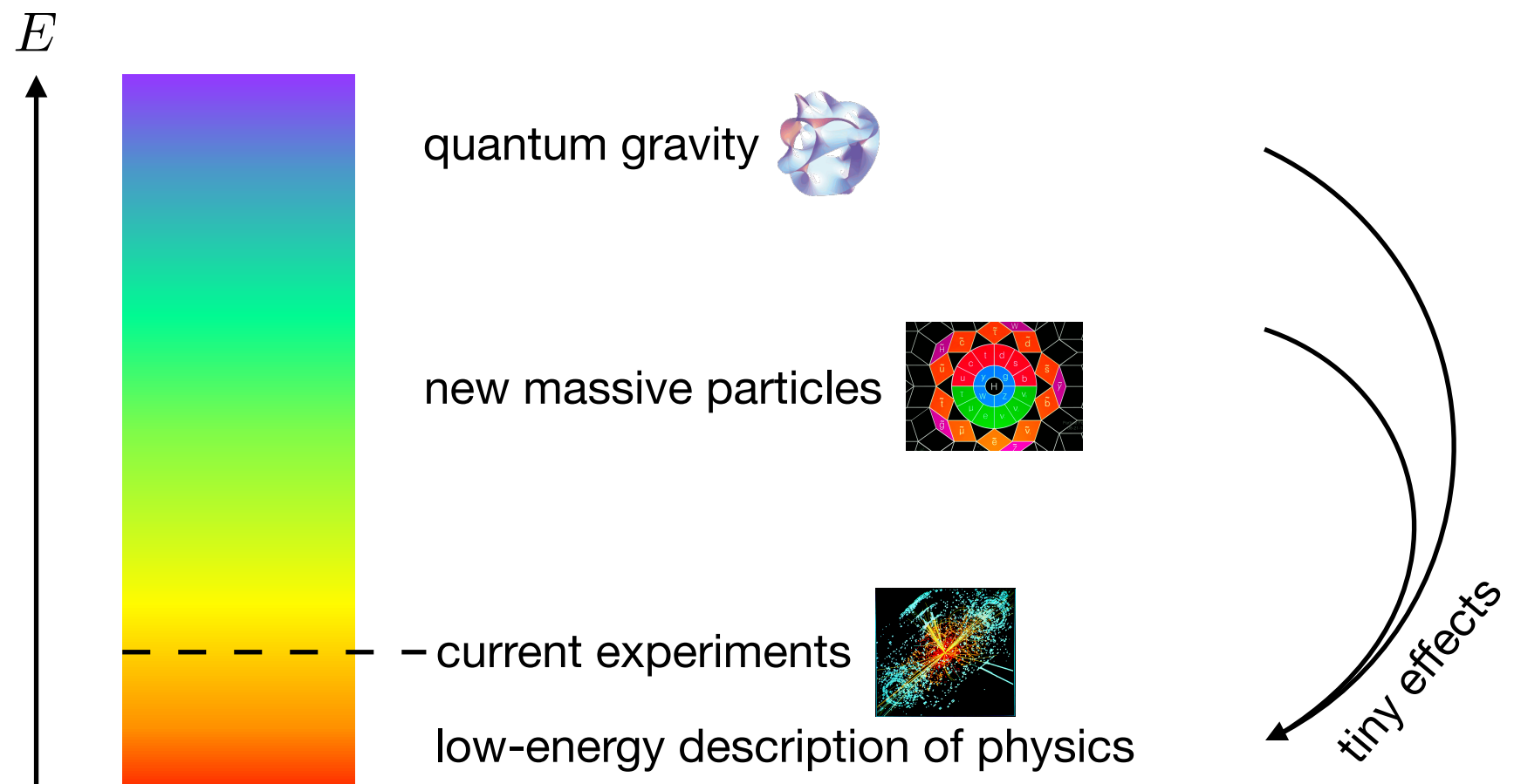
Introduction

Effective field theory

How do we encode hints of ultraviolet physics in the infrared?

Effective field theory

How do we encode hints of ultraviolet physics in the infrared?



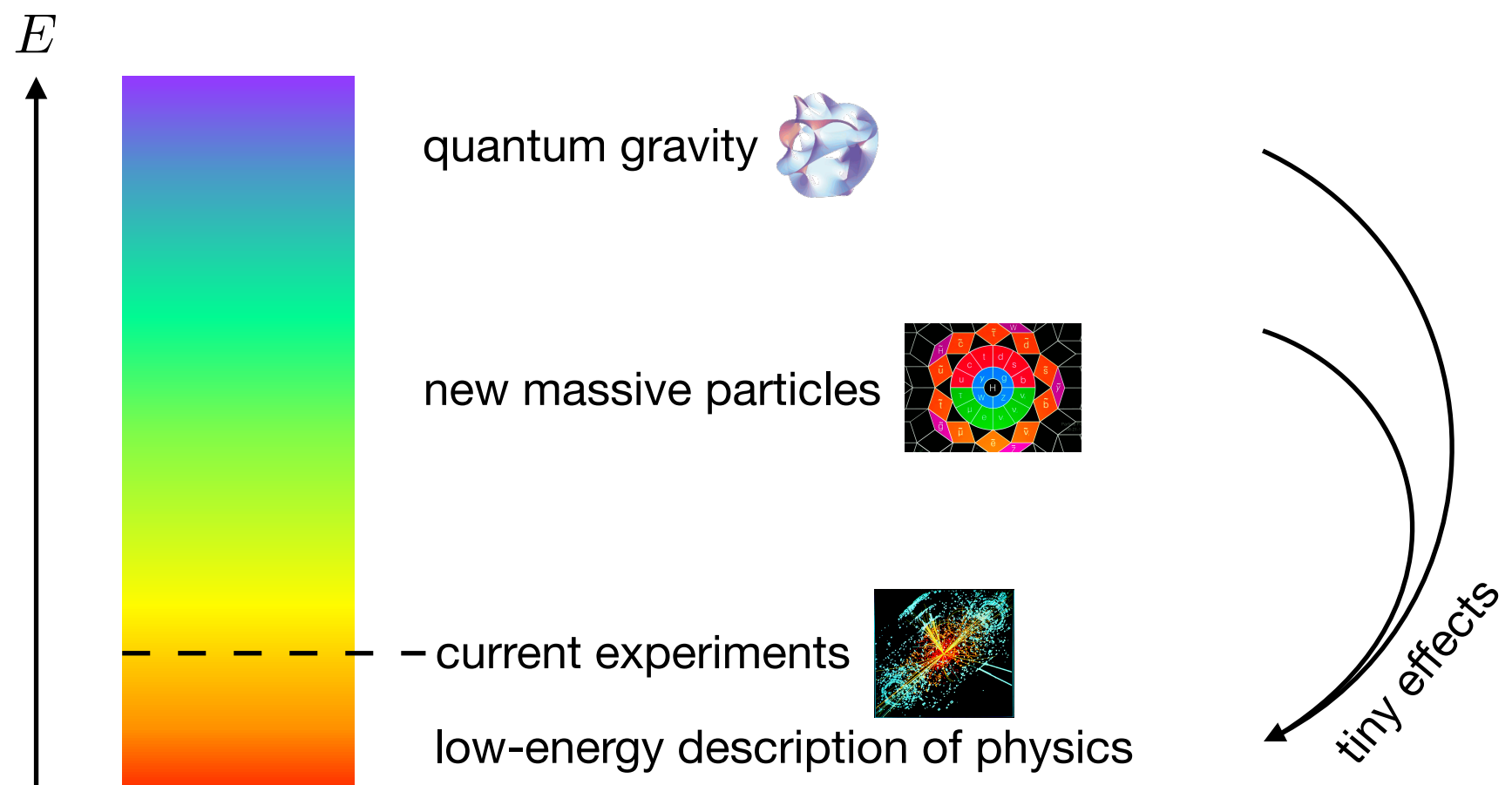
Effective field theory

How do we encode hints of ultraviolet physics in the infrared?

- Write down a Lagrangian, built out of operators \mathcal{O}_i , with couplings c_i :

$$\mathcal{L} = \bar{\mathcal{L}} + \sum_i c_i \mathcal{O}_i$$

including all possible operators consistent with the fields and symmetries.



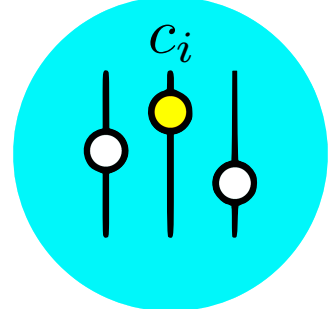
Effective field theory

How do we encode hints of ultraviolet physics in the infrared?

- Write down a Lagrangian, built out of operators \mathcal{O}_i , with couplings c_i :

$$\mathcal{L} = \bar{\mathcal{L}} + \sum_i c_i \mathcal{O}_i$$

↑ ↑
Einstein-Hilbert term Higher-derivative operators



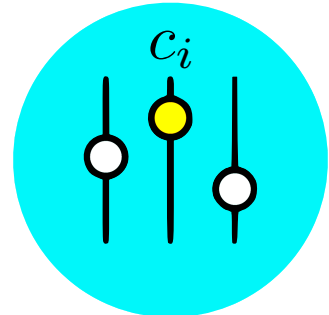
Effective field theory

How do we encode hints of ultraviolet physics in the infrared?

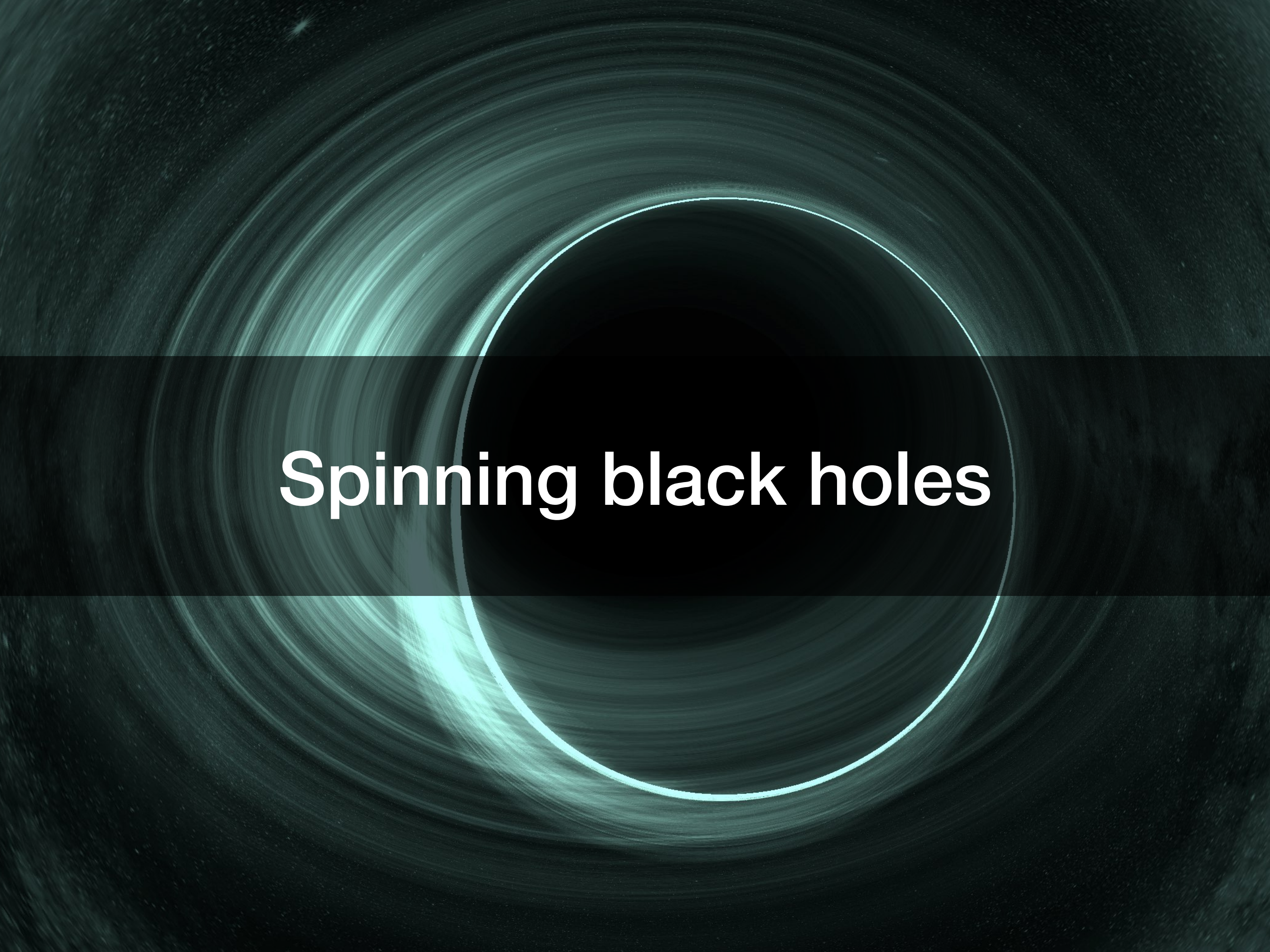
- Write down a Lagrangian, built out of operators \mathcal{O}_i , with couplings c_i :

$$\mathcal{L} = \bar{\mathcal{L}} + \sum_i c_i \mathcal{O}_i$$

↑ ↑
Einstein-Hilbert term Higher-derivative operators



- The famous nonrenormalizability of perturbative quantum gravity is now well understood as a manifestation of the fact that GR is itself an effective field theory.
- Higher-derivative terms are generated by the UV completion, and are suppressed by either the Planck scale or the scale of massive degrees of freedom. Run from loops of light states (gravitons, photons, etc.).

A black hole is shown against a dark background. It has a bright, glowing blue-green accretion disk surrounding it. The disk is most intense at the edges and tapers off towards the center. The black hole itself is a solid black circle in the center of the disk.

Spinning black holes

Kerr solution

- The Kerr geometry solves the vacuum Einstein equations (i.e., it is Ricci-flat) and describes a spinning black hole:

$$\begin{aligned} ds_K^2 = & -\frac{\Delta(r)}{\Sigma(r, \theta)}(dt - a \sin^2 \theta d\phi)^2 + \Sigma(r, \theta) \left(\frac{dr^2}{\Delta(r)} + d\theta^2 \right) \\ & + \frac{\sin^2 \theta}{\Sigma(r, \theta)} [a dt - (r^2 + a^2)d\phi]^2 \\ \Sigma(r, \theta) = & r^2 + a^2 \cos^2 \theta \\ \Delta(r) = & r^2 + a^2 - 2Mr \quad a = GJ/M \end{aligned}$$

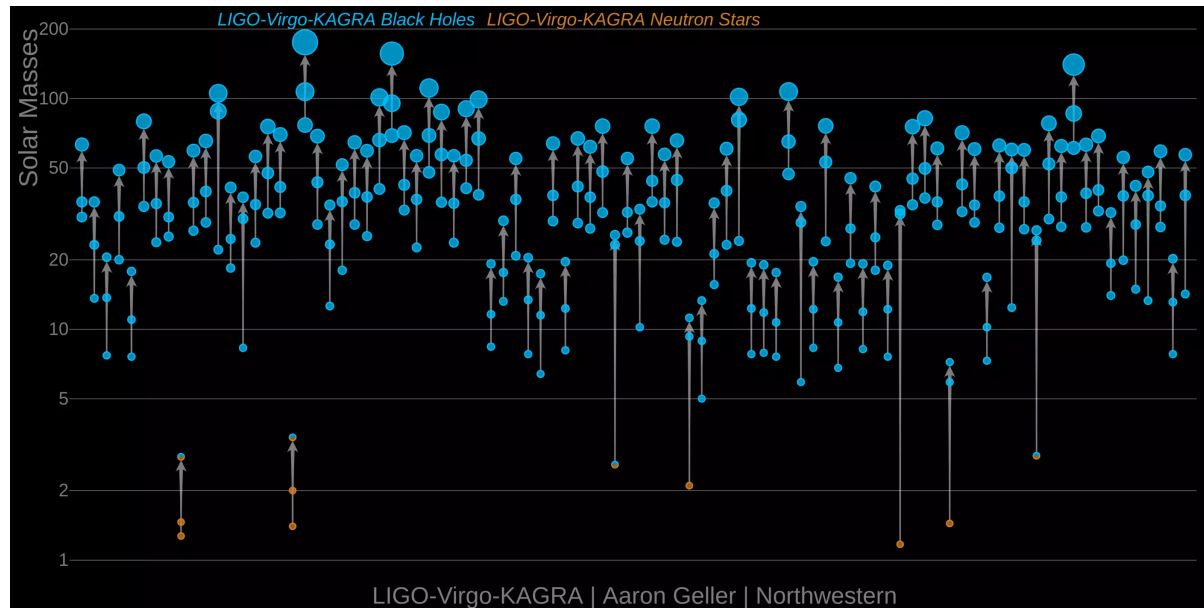
- Event horizon at $r_+ = M + \sqrt{M^2 - a^2}$

Kerr solution

- The Kerr geometry solves the vacuum Einstein equations (i.e., it is Ricci-flat) and describes a spinning black hole:

$$\begin{aligned} ds_K^2 = & -\frac{\Delta(r)}{\Sigma(r, \theta)}(dt - a \sin^2 \theta d\phi)^2 + \Sigma(r, \theta) \left(\frac{dr^2}{\Delta(r)} + d\theta^2 \right) \\ & + \frac{\sin^2 \theta}{\Sigma(r, \theta)} [a dt - (r^2 + a^2)d\phi]^2 \\ \Sigma(r, \theta) = & r^2 + a^2 \cos^2 \theta \\ \Delta(r) = & r^2 + a^2 - 2Mr \quad a = GJ/M \end{aligned}$$

- Event horizon at $r_+ = M + \sqrt{M^2 - a^2}$
- No Birkhoff theorem: exterior spacetime rotating matter is generally not Kerr.
- Many likely examples observed by LIGO:



NHEK

In the extremal limit, the Kerr geometry has an infinitely long throat near the horizon, the near-horizon extremal Kerr (NHEK) geometry:



$$ds_{\text{NHEK}}^2 = J(1 + x^2) \left[-\rho^2 dt^2 + \frac{d\rho^2}{\rho^2} + \frac{dx^2}{1 - x^2} + \frac{2(1 - x^2)}{(1 + x^2)^2} (d\phi + \rho dt)^2 \right]$$

Bardeen, Horowitz [hep-th/9905099]

- Similar to $\text{AdS}_2 \times S^2$, with $O(2, 1) \times U(1)$ symmetry

ρ



to horizon at $\rho = 0$

NHEK

In the extremal limit, the Kerr geometry has an infinitely long throat near the horizon, the near-horizon extremal Kerr (NHEK) geometry:



$$ds_{\text{NHEK}}^2 = J(1+x^2) \left[-\rho^2 dt^2 + \frac{d\rho^2}{\rho^2} + \frac{dx^2}{1-x^2} + \frac{2(1-x^2)}{(1+x^2)^2} (d\phi + \rho dt)^2 \right]$$

Bardeen, Horowitz [hep-th/9905099]

- Similar to $\text{AdS}_2 \times S^2$, with $O(2, 1) \times U(1)$ symmetry
- First correction around NHEK patching onto asymptotically flat Kerr geometry can be understood as coming from certain modes of the linearized Einstein equations in the NHEK background [cf. Hadar, Lupsasca, Porfyriadis \[2012.06562\]](#)
- Of great interest to Kerr-CFT proposals
[Guica, Hartman, Song, Strominger \[0809.4266\]](#)

to horizon at $\rho = 0$

NHEK

In the extremal limit, the Kerr geometry has an infinitely long throat near the horizon, the near-horizon extremal Kerr (NHEK) geometry:


 (θ, ϕ)

$$ds_{\text{NHEK}}^2 = J(1+x^2) \left[-\rho^2 dt^2 + \frac{d\rho^2}{\rho^2} + \frac{dx^2}{1-x^2} + \frac{2(1-x^2)}{(1+x^2)^2} (d\phi + \rho dt)^2 \right]$$

Bardeen, Horowitz [hep-th/9905099]

- Similar to $\text{AdS}_2 \times S^2$, with $O(2, 1) \times U(1)$ symmetry
- First correction around NHEK patching onto asymptotically flat Kerr geometry can be understood as coming from certain modes of the linearized Einstein equations in the NHEK background cf. Hadar, Lupsasca, Porfyriadis [2012.06562]
- Of great interest to Kerr-CFT proposals
Guica, Hartman, Song, Strominger [0809.4266]
- We will determine the near-horizon behavior of the EFT-corrected Kerr geometry by computing EFT corrections to the NHEK.

to horizon at $\rho = 0$

EFT in vacuum

- Let us first consider the gravitational EFT where no matter is present.
- We must build the EFT out of the Riemann tensor, with no contractions. Any appearance of the Ricci tensor can be removed via field redefinitions.

EFT in vacuum

- Let us first consider the gravitational EFT where no matter is present.
- We must build the EFT out of the Riemann tensor, with no contractions. Any appearance of the Ricci tensor can be removed via field redefinitions.
- In four spacetime dimensions, the Gauss-Bonnet term is topological:

$$\begin{aligned} & \int d^4x \sqrt{-g} (R_{abcd}R^{abcd} - 4R_{ab}R^{ab} + R^2) \\ &= \int d^4x \partial_a \left[\sqrt{-g} \epsilon^{abcd} \epsilon_{ef}{}^{gh} \Gamma_{gb}^e \left(\frac{1}{2} R^f{}_{hcd} - \frac{1}{3} \Gamma_{ci}^f \Gamma_{hd}^i \right) \right] \\ &= 8\pi^2 \chi(\mathcal{M}) \end{aligned}$$

EFT in vacuum

- Let us first consider the gravitational EFT where no matter is present.
- We must build the EFT out of the Riemann tensor, with no contractions. Any appearance of the Ricci tensor can be removed via field redefinitions.
- In four spacetime dimensions, the Gauss-Bonnet term is topological:

$$\begin{aligned} & \int d^4x \sqrt{-g} (R_{abcd}R^{abcd} - 4R_{ab}R^{ab} + R^2) \\ &= \int d^4x \partial_a \left[\sqrt{-g} \epsilon^{abcd} \epsilon_{ef}{}^{gh} \Gamma_{gb}^e \left(\frac{1}{2} R^f{}_{hcd} - \frac{1}{3} \Gamma_{ci}^f \Gamma_{hd}^i \right) \right] \\ &= 8\pi^2 \chi(\mathcal{M}) \end{aligned}$$

- First interesting terms at cubic and quartic order in the Riemann tensor:

$$\mathcal{L} = \frac{1}{2\kappa^2} \left(R + \eta \kappa^4 \mathcal{R}^3 + \lambda \kappa^6 \mathcal{C}^2 + \tilde{\lambda} \kappa^6 \tilde{\mathcal{C}}^2 \right)$$

$$\mathcal{R}^3 = R_{ab}{}^{cd} R_{cd}{}^{ef} R_{ef}{}^{ab}$$

$$\mathcal{C} = R_{abcd} R^{abcd}$$

$$\tilde{\mathcal{C}} = \tilde{R}_{abcd} R^{abcd}$$

$$\tilde{R}_{abcd} = \epsilon_{ab}{}^{ef} R_{efcd}$$

EFT in vacuum

- Classical equations of motion:

$$R_{ab} - \frac{1}{2} R g_{ab} = T_{ab}^{\text{cubic}} + T_{ab}^{\text{quartic}}$$

$$T_{ab}^{\text{cubic}} = \eta \kappa^4 \left[3 R_a{}^{cde} R_{de}{}^{gh} R_{ghcb} + \frac{1}{2} g_{ab} R_{gh}{}^{cd} R_{cd}{}^{ef} R_{ef}{}^{gh} - 6 \nabla^c \nabla^d \left(R_{acgh} R_{bd}{}^{gh} \right) \right]$$

$$T_{ab}^{\text{quartic}} = -\lambda \kappa^6 \left(8 R_{acbd} \nabla^c \nabla^d \mathcal{C} + \frac{g_{ab}}{2} \mathcal{C}^2 \right) - \tilde{\lambda} \kappa^6 \left(8 \tilde{R}_{acbd} \nabla^c \nabla^d \tilde{\mathcal{C}} + \frac{g_{ab}}{2} \tilde{\mathcal{C}}^2 \right)$$

EFT in vacuum

- Classical equations of motion:

$$R_{ab} - \frac{1}{2} R g_{ab} = T_{ab}^{\text{cubic}} + T_{ab}^{\text{quartic}}$$

$$T_{ab}^{\text{cubic}} = \eta \kappa^4 \left[3 R_a^{cde} R_{de}^{gh} R_{ghcb} + \frac{1}{2} g_{ab} R_{gh}^{cd} R_{cd}^{ef} R_{ef}^{gh} - 6 \nabla^c \nabla^d \left(R_{acgh} R_{bd}^{gh} \right) \right]$$

$$T_{ab}^{\text{quartic}} = -\lambda \kappa^6 \left(8 R_{acbd} \nabla^c \nabla^d \mathcal{C} + \frac{g_{ab}}{2} \mathcal{C}^2 \right) - \tilde{\lambda} \kappa^6 \left(8 \tilde{R}_{acbd} \nabla^c \nabla^d \tilde{\mathcal{C}} + \frac{g_{ab}}{2} \tilde{\mathcal{C}}^2 \right)$$

- Solve at linear order in the Wilson coefficients,

$$g_{ab} = g_{ab}^{(0)} + \eta h_{ab}^{(6)} + \lambda h_{ab}^{(8)} + \tilde{\lambda} \tilde{h}_{ab}^{(8)}$$

EFT in vacuum

- Classical equations of motion:

$$R_{ab} - \frac{1}{2} R g_{ab} = T_{ab}^{\text{cubic}} + T_{ab}^{\text{quartic}}$$

$$T_{ab}^{\text{cubic}} = \eta \kappa^4 \left[3 R_a^{cde} R_{de}^{gh} R_{ghcb} + \frac{1}{2} g_{ab} R_{gh}^{cd} R_{cd}^{ef} R_{ef}^{gh} - 6 \nabla^c \nabla^d \left(R_{acgh} R_{bd}^{gh} \right) \right]$$

$$T_{ab}^{\text{quartic}} = -\lambda \kappa^6 \left(8 R_{acbd} \nabla^c \nabla^d \mathcal{C} + \frac{g_{ab}}{2} \mathcal{C}^2 \right) - \tilde{\lambda} \kappa^6 \left(8 \tilde{R}_{acbd} \nabla^c \nabla^d \tilde{\mathcal{C}} + \frac{g_{ab}}{2} \tilde{\mathcal{C}}^2 \right)$$

- Solve at linear order in the Wilson coefficients,

$$g_{ab} = g_{ab}^{(0)} + \eta h_{ab}^{(6)} + \lambda h_{ab}^{(8)} + \tilde{\lambda} \tilde{h}_{ab}^{(8)}$$

- $\mathcal{O}(\eta^2)$ contribution $\delta h_{ab}^{(6)}$ to $h_{ab}^{(6)}$ is smaller than $h_{ab}^{(8)}$:
By power counting and the form of the equations of motion,

$$(\delta h_{ab}^{(6)})/(h_{ab}^{(8)}) \sim (\eta^2/\lambda)(\kappa^2/J)$$

Indeed, by [Caron-Huot, Li, Parra-Martinez, Simmons-Duffin \[2201.06602\]](#), we expect $\eta^2/\lambda \lesssim m_{\text{Pl}}^2/\Lambda_{\text{UV}}^2$

EFT-corrected NHEK geometry

- Stationary, axisymmetric ansatz:

$$ds^2 = 2J\Omega^2 \left[-\rho^2 dt^2 + \frac{F_1}{\rho^2} (d\rho + \rho F_2 dx)^2 + \frac{dx^2}{A} + B^2 (d\phi + \rho\omega dt)^2 \right]$$

- Fix gauge: $F_1 = 1$ and $F_2 = 0$

EFT-corrected NHEK geometry

- Stationary, axisymmetric ansatz:

$$ds^2 = 2J\Omega^2 \left[-\rho^2 dt^2 + \frac{F_1}{\rho^2} (\mathrm{d}\rho + \rho F_2 \mathrm{d}x)^2 + \frac{\mathrm{d}x^2}{A} + B^2 (\mathrm{d}\phi + \rho\omega \mathrm{d}t)^2 \right]$$

- Fix gauge: $F_1 = 1$ and $F_2 = 0$
- Impose $O(2, 1) \times U(1)$ symmetry,

$$\Omega = \Omega_{\text{NH}}(x)$$

$$B = B_{\text{NH}}(x)$$

$$A = \frac{1 - x^2}{\Gamma_{\text{NH}}^2}$$

$$\Gamma_{\text{NH}} = \text{const.}$$

$$\omega = \omega_{\text{NH}} = \text{const.}$$

so that the ansatz becomes:

$$ds^2 = 2J\Omega_{\text{NH}}^2 \left[-\rho^2 dt^2 + \frac{\mathrm{d}\rho^2}{\rho^2} + \frac{\Gamma_{\text{NH}}^2 \mathrm{d}x^2}{1 - x^2} + B_{\text{NH}}^2 (\mathrm{d}\phi + \rho\omega_{\text{NH}} \mathrm{d}t)^2 \right]$$

EFT-corrected NHEK geometry

$$ds^2 = 2J\Omega_{\text{NH}}^2 \left[-\rho^2 dt^2 + \frac{d\rho^2}{\rho^2} + \frac{\Gamma_{\text{NH}}^2 dx^2}{1-x^2} + B_{\text{NH}}^2 (d\phi + \rho\omega_{\text{NH}} dt)^2 \right]$$

- Expand around NHEK solution:

$$\Omega_{\text{NH}} = \sqrt{\frac{1+x^2}{2}} \left[1 + \eta\Omega^{(6)}(x) + \lambda\Omega^{(8)}(x) + \tilde{\lambda}\tilde{\Omega}^{(8)}(x) \right]$$

$$B_{\text{NH}} = \frac{2\sqrt{1-x^2}}{1+x^2} \left[1 + \eta B^{(6)}(x) + \lambda B^{(8)}(x) + \tilde{\lambda}\tilde{B}^{(8)}(x) \right]$$

$$\Gamma_{\text{NH}} = 1 + \eta\Gamma^{(6)}(x) + \lambda\Gamma^{(8)}(x) + \tilde{\lambda}\tilde{\Gamma}^{(8)}(x)$$

$$\omega_{\text{NH}} = 1 + \eta\omega^{(6)}(x) + \lambda\omega^{(8)}(x) + \tilde{\lambda}\tilde{\omega}^{(8)}(x)$$

EFT-corrected NHEK geometry

$$ds^2 = 2J\Omega_{\text{NH}}^2 \left[-\rho^2 dt^2 + \frac{d\rho^2}{\rho^2} + \frac{\Gamma_{\text{NH}}^2 dx^2}{1-x^2} + B_{\text{NH}}^2 (d\phi + \rho\omega_{\text{NH}} dt)^2 \right]$$

- Expand around NHEK solution:

$$\Omega_{\text{NH}} = \sqrt{\frac{1+x^2}{2}} \left[1 + \eta\Omega^{(6)}(x) + \lambda\Omega^{(8)}(x) + \tilde{\lambda}\tilde{\Omega}^{(8)}(x) \right]$$

$$B_{\text{NH}} = \frac{2\sqrt{1-x^2}}{1+x^2} \left[1 + \eta B^{(6)}(x) + \lambda B^{(8)}(x) + \tilde{\lambda}\tilde{B}^{(8)}(x) \right]$$

$$\Gamma_{\text{NH}} = 1 + \eta\Gamma^{(6)}(x) + \lambda\Gamma^{(8)}(x) + \tilde{\lambda}\tilde{\Gamma}^{(8)}(x)$$

$$\omega_{\text{NH}} = 1 + \eta\omega^{(6)}(x) + \lambda\omega^{(8)}(x) + \tilde{\lambda}\tilde{\omega}^{(8)}(x)$$

- Solving the equations of motion, we find:

$$\Gamma^{(6)} = -\frac{15\kappa^4}{32\sqrt{2}J^2}$$

$$\omega^{(6)} = \frac{\kappa^4}{7J^2}$$

$$\Gamma^{(8)} = -\frac{366435\kappa^6}{256\sqrt{2}J^3}$$

$$\omega^{(8)} = \frac{(4864 + 1575\pi)\kappa^6}{20J^3}$$

$$\tilde{\Gamma}^{(8)} = -\frac{368829\kappa^6}{64\sqrt{2}J^3}$$

$$\tilde{\omega}^{(8)} = \frac{(4736 + 1575\pi)\kappa^6}{5J^3}$$

EFT-corrected NHEK geometry

$$ds^2 = 2J\Omega_{\text{NH}}^2 \left[-\rho^2 dt^2 + \frac{d\rho^2}{\rho^2} + \frac{\Gamma_{\text{NH}}^2 dx^2}{1-x^2} + B_{\text{NH}}^2 (d\phi + \rho\omega_{\text{NH}} dt)^2 \right]$$

- Solving the equations of motion, we find:

$$B^{(6)}(x) = \frac{\kappa^4}{J^2} \left[\frac{2656 - 42885x^2 + 45895x^4 - 8130x^6 - 1218x^8 + 183x^{10} + 139x^{12}}{224(1+x^2)^6} \right. \\ \left. - \frac{15\sqrt{2}x(3-x^2)}{64(1+x^2)\sqrt{1-x^2}} \left(\arcsin \frac{\sqrt{2}x}{\sqrt{1+x^2}} - \arcsin x \right) \right]$$

$$\Omega^{(6)}(x) = \frac{\kappa^4}{J^2} \left[C^{(6)} - \frac{3285 - 55449x^2 + 54210x^4 - 7058x^6 - 1527x^8 - 309x^{10}}{224(1+x^2)^6} \right. \\ \left. + \frac{15x\sqrt{2}\sqrt{1-x^2}}{64(1+x^2)} \left(\arcsin \frac{\sqrt{2}x}{\sqrt{1+x^2}} - \arcsin x \right) \right]$$

EFT-corrected NHEK geometry

$$ds^2 = 2J\Omega_{\text{NH}}^2 \left[-\rho^2 dt^2 + \frac{d\rho^2}{\rho^2} + \frac{\Gamma_{\text{NH}}^2 dx^2}{1-x^2} + B_{\text{NH}}^2 (d\phi + \rho\omega_{\text{NH}} dt)^2 \right]$$

- Solving the equations of motion, we find:

$$\begin{aligned} B^{(8)}(x) = & \frac{\kappa^6}{J^3} \left[\frac{832989}{1280} - \frac{315\pi}{4} - \frac{407005 + 32887800x^2 + 38302380x^4 + 227158536x^6}{1280(1+x^2)^9} \right. \\ & - \frac{244951182x^8 + 207667400x^{10} + 108083820x^{12} + 31954360x^{14} + 4114685x^{16}}{1280(1+x^2)^9} \\ & \left. + \frac{630x}{(1+x^2)} \arctan x - \frac{366435x(3-x^2)}{256\sqrt{2}\sqrt{1-x^2}(1+x^2)} \left(\arcsin \frac{\sqrt{2}x}{\sqrt{1+x^2}} - \arcsin x \right) \right] \end{aligned}$$

$$\begin{aligned} \Omega^{(8)}(x) = & \frac{\kappa^6}{J^3} \left[C^{(8)} + \frac{783837 + 16684758x^2 + 33602022x^4 + 119986542x^6}{1280(1+x^2)^9} \right. \\ & + \frac{27639936x^8 + 23049562x^{10} + 11880370x^{12} + 3484978x^{14} + 445863x^{16}}{256(1+x^2)^9} \\ & \left. - \frac{315x}{1+x^2} \arctan x + \frac{366435x\sqrt{1-x^2}}{256\sqrt{2}(1+x^2)} \left(\arcsin \frac{\sqrt{2}x}{\sqrt{1+x^2}} - \arcsin x \right) \right] \end{aligned}$$

EFT-corrected NHEK geometry

$$ds^2 = 2J\Omega_{\text{NH}}^2 \left[-\rho^2 dt^2 + \frac{d\rho^2}{\rho^2} + \frac{\Gamma_{\text{NH}}^2 dx^2}{1-x^2} + B_{\text{NH}}^2 (d\phi + \rho\omega_{\text{NH}} dt)^2 \right]$$

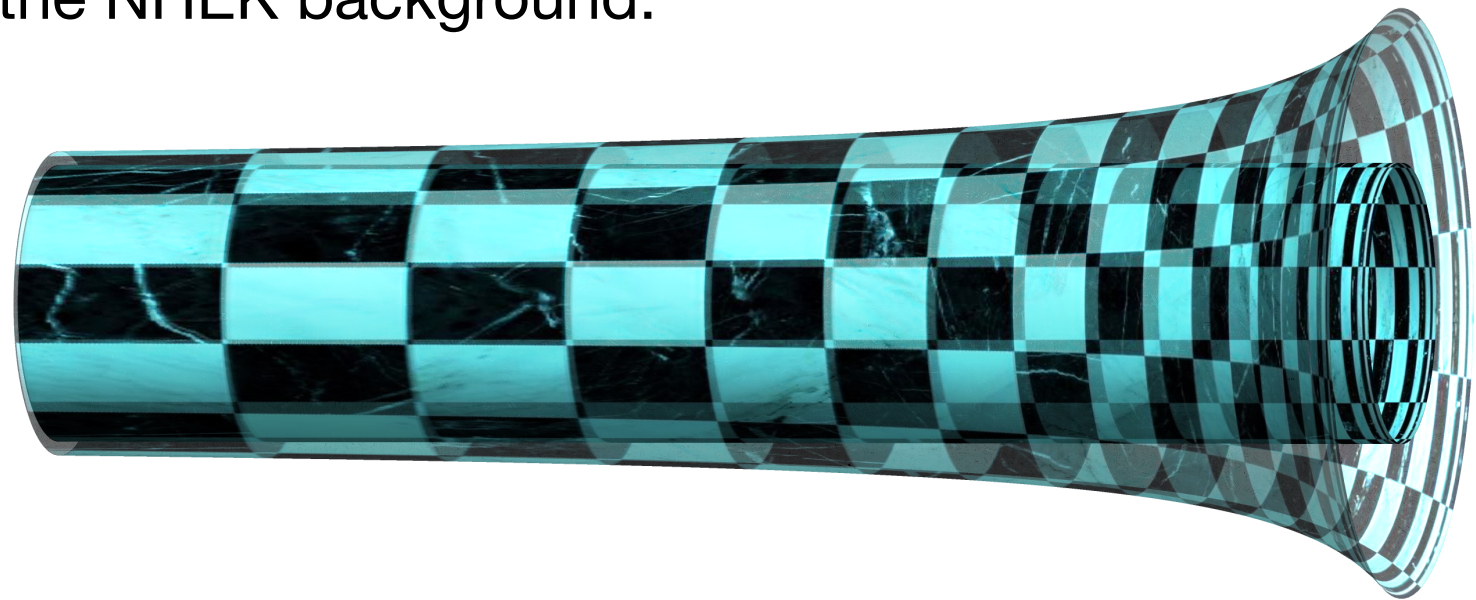
- Solving the equations of motion, we find:

$$\begin{aligned} \tilde{B}^{(8)}(x) = & \frac{\kappa^6}{J^3} \left[\frac{846339}{320} - 315\pi - \frac{1149443+5618952x^2+136013268x^4+154320120x^6+254641842x^8}{320(1+x^2)^9} \right. \\ & - \frac{208733752x^{10} + 108674580x^{12} + 32136008x^{14} + 4138723x^{16}}{320(1+x^2)^9} \\ & \left. + \frac{2520x}{1+x^2} \arctan x - \frac{368829x(3-x^2)}{64\sqrt{2}\sqrt{1-x^2}(1+x^2)} \left(\arcsin \frac{\sqrt{2}x}{\sqrt{1+x^2}} - \arcsin x \right) \right] \end{aligned}$$

$$\begin{aligned} \tilde{\Omega}^{(8)}(x) = & \frac{\kappa^6}{J^3} \left[\tilde{C}^{(8)} + \frac{1018371+7724394x^2+67516506x^4+96062418x^6+141833088x^8}{320(1+x^2)^9} \right. \\ & + \frac{115923454x^{10} + 59757382x^{12} + 17530822x^{14} + 2243037x^{16}}{320(1+x^2)^9} \\ & \left. - \frac{1260x}{1+x^2} \arctan x + \frac{368829x\sqrt{1-x^2}}{64\sqrt{2}(1+x^2)} \left(\arcsin \frac{\sqrt{2}x}{\sqrt{1+x^2}} - \arcsin x \right) \right] \end{aligned}$$

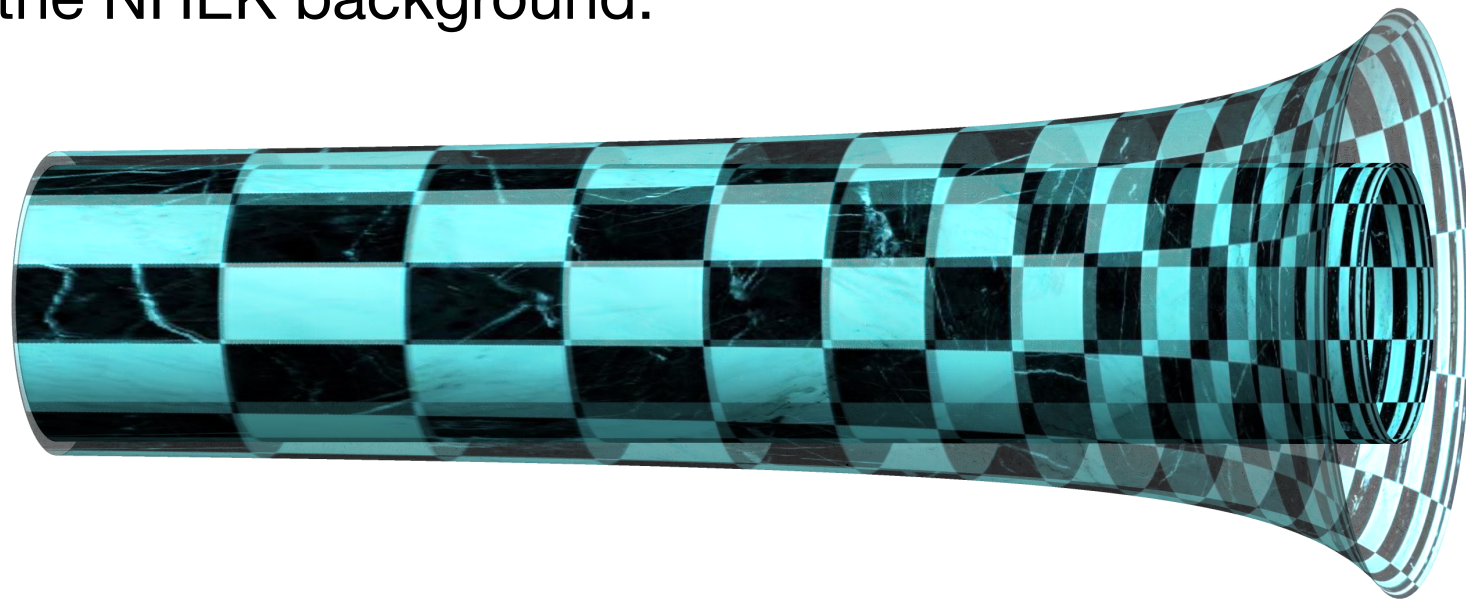
Perturbing the NHEK geometry

- Patching the near-horizon geometry to asymptotically flat Kerr solution can be thought of as inducing some perturbative mode solving the linearized Einstein equation in the NHEK background:



Perturbing the NHEK geometry

- Patching the near-horizon geometry to asymptotically flat Kerr solution can be thought of as inducing some perturbative mode solving the linearized Einstein equation in the NHEK background:



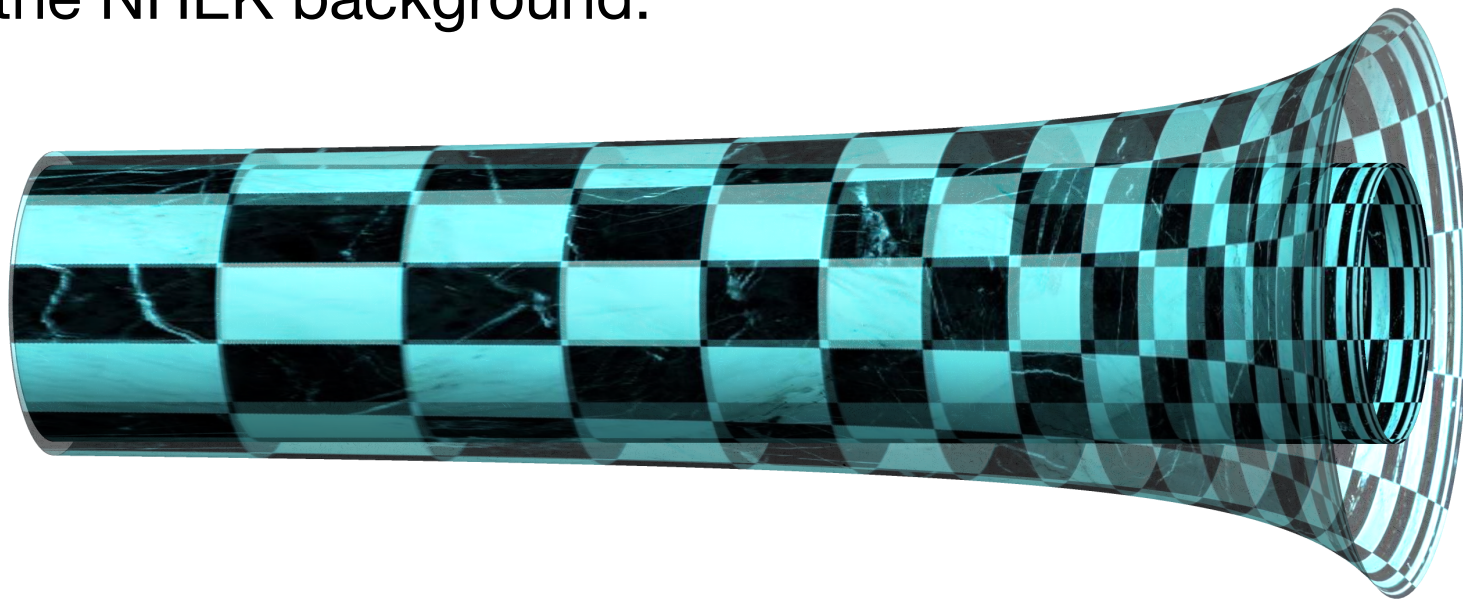
- Let us see how this works explicitly for Kerr/NHEK, before repeating the calculation with EFT corrections. We start with the ansatz,

$$ds^2 = 2J\Omega^2 \left[-\rho^2 dt^2 + \frac{F_1}{\rho^2} (d\rho + \rho F_2 dx)^2 + \frac{dx^2}{A} + B^2 (d\phi + \rho\omega dt)^2 \right]$$

with gauge choice $F_1 = 1, F_2 = 0$.

Perturbing the NHEK geometry

- Patching the near-horizon geometry to asymptotically flat Kerr solution can be thought of as inducing some perturbative mode solving the linearized Einstein equation in the NHEK background:



- Let us see how this works explicitly for Kerr/NHEK, before repeating the calculation with EFT corrections. We start with the ansatz,

$$ds^2 = 2J\Omega^2 \left[-\rho^2 dt^2 + \frac{F_1}{\rho^2} (d\rho + \rho F_2 dx)^2 + \frac{dx^2}{A} + B^2 (d\phi + \rho\omega dt)^2 \right]$$

with gauge choice $F_1 = 1, F_2 = 0$.

Decompose stationary, axisymmetric perturbations into **AdS₂ harmonics** $\sim \rho^\gamma$:

$$A(\rho, x) = A_{\text{NH}}(x) [1 + \varepsilon \rho^\gamma Q_1(x)]$$

$$B(\rho, x) = B_{\text{NH}}(x) [1 + \varepsilon \rho^\gamma Q_2(x)]$$

$$\Omega(\rho, x) = \Omega_{\text{NH}}(x) [1 + \varepsilon \rho^\gamma Q_3(x)]$$

$$\omega(\rho, x) = \omega_{\text{NH}} [1 + \varepsilon \rho^\gamma Q_4(x)]$$

Perturbing the NHEK geometry

- Expand in Wilson coefficients:

$$Q_i(x) = Q_i^{(0)}(x) + \eta Q_i^{(6)}(x) + \lambda Q_i^{(8)}(x) + \tilde{\lambda} \tilde{Q}_i^{(8)}(x)$$
$$\gamma = \gamma^{(0)} + \eta \gamma^{(6)} + \lambda \gamma^{(8)} + \tilde{\lambda} \tilde{\gamma}^{(8)}$$

Perturbing the NHEK geometry

- Expand in Wilson coefficients:

$$Q_i(x) = Q_i^{(0)}(x) + \eta Q_i^{(6)}(x) + \lambda Q_i^{(8)}(x) + \tilde{\lambda} \tilde{Q}_i^{(8)}(x)$$
$$\gamma = \gamma^{(0)} + \eta \gamma^{(6)} + \lambda \gamma^{(8)} + \tilde{\lambda} \tilde{\gamma}^{(8)}$$

- Second-order equations yield two families of solutions:

$$Q_1^{(0)+}(x) = P'_\ell(x)$$
$$Q_2^{(0)+}(x) = -\frac{1}{2(1+x^2)} \left[2\ell(\ell+1)xP_\ell(x) + (1-3x^2)P'_\ell(x) \right]$$
$$Q_3^{(0)+}(x) = \frac{1}{2(1+x^2)} \left[\ell(\ell+1)xP_\ell(x) + (1-x^2)P'_\ell(x) \right] \quad \ell \geq 2$$
$$Q_4^{(0)+}(x) = \frac{1}{2} \left[\ell x P_\ell(x) + \frac{(1-x^2)(\ell^2+\ell+2)}{2(\ell+1)} P'_\ell(x) \right]$$

Perturbing the NHEK geometry

- Expand in Wilson coefficients:

$$Q_i(x) = Q_i^{(0)}(x) + \eta Q_i^{(6)}(x) + \lambda Q_i^{(8)}(x) + \tilde{\lambda} \tilde{Q}_i^{(8)}(x)$$
$$\gamma = \gamma^{(0)} + \eta \gamma^{(6)} + \lambda \gamma^{(8)} + \tilde{\lambda} \tilde{\gamma}^{(8)}$$

- Second-order equations yield two families of solutions:

$$Q_1^{(0)-}(x) = 0$$

$$Q_2^{(0)-}(x) = \frac{1-x^2}{1+x^2} \left\{ \ell(\ell+1) x P_\ell(x) - [2 + (1-x^2)\ell] P'_\ell(x) \right\}$$

$$Q_3^{(0)-}(x) = -\frac{1}{2} \frac{1-x^2}{1+x^2} \left\{ \ell(\ell+1) x P_\ell(x) - [2 + (1-x^2)\ell] P'_\ell(x) \right\} \quad \ell \geq 1$$

$$Q_4^{(0)-}(x) = \ell(\ell+1) x P_\ell(x) + (1+x^2\ell) P'_\ell(x)$$

Perturbing the NHEK geometry

- Expand in Wilson coefficients:

$$Q_i(x) = Q_i^{(0)}(x) + \eta Q_i^{(6)}(x) + \lambda Q_i^{(8)}(x) + \tilde{\lambda} \tilde{Q}_i^{(8)}(x)$$
$$\gamma = \gamma^{(0)} + \eta \gamma^{(6)} + \lambda \gamma^{(8)} + \tilde{\lambda} \tilde{\gamma}^{(8)}$$

- Second-order equations yield two families of solutions:

$$\gamma_+^{(0)}(\ell) = \ell \quad \text{with} \quad \ell \in \mathbb{N} \geq 2$$

$$\gamma_-^{(0)}(\ell) = \ell + 1 \quad \text{with} \quad \ell \in \mathbb{N} \geq 1$$

Perturbing the NHEK geometry

- Expand in Wilson coefficients:

$$Q_i(x) = Q_i^{(0)}(x) + \eta Q_i^{(6)}(x) + \lambda Q_i^{(8)}(x) + \tilde{\lambda} \tilde{Q}_i^{(8)}(x)$$

$$\gamma = \gamma^{(0)} + \eta \gamma^{(6)} + \lambda \gamma^{(8)} + \tilde{\lambda} \tilde{\gamma}^{(8)}$$

- Second-order equations yield two families of solutions:

$$\gamma_+^{(0)}(\ell) = \ell \quad \text{with} \quad \ell \in \mathbb{N} \geq 2$$

$$\gamma_-^{(0)}(\ell) = \ell + 1 \quad \text{with} \quad \ell \in \mathbb{N} \geq 1$$

- Integer scaling dimensions ≥ 2 correspond to smooth horizons. For example, we can compute the Weyl curvature in ingoing Bondi-Sachs coordinates:

$$ds^2 = 2J\Omega^2 [-\rho^2 dv^2 + 2dv d\rho + h_{ab}(dy^a + U^a dv)(dy^b + U^b dv)]$$

Mapping to our other coordinates, we have:

$$C_{\rho a \rho b} = J(1-\gamma) \rho^{\gamma-2} \varepsilon \begin{bmatrix} -\frac{\gamma \Gamma_{\text{NH}}^2 (Q_1 + 2Q_2) \Omega_{\text{NH}}^2}{2(1-x^2)} & B_{\text{NH}}^2 \Omega_{\text{NH}}^2 Q'_4 \\ B_{\text{NH}}^2 \Omega_{\text{NH}}^2 Q'_4 & -\frac{\gamma B_{\text{NH}}^2 (Q_1 + 2Q_2) \Omega_{\text{NH}}^2}{2} \end{bmatrix}$$

Perturbing the NHEK geometry

- Expand in Wilson coefficients:

$$Q_i(x) = Q_i^{(0)}(x) + \eta Q_i^{(6)}(x) + \lambda Q_i^{(8)}(x) + \tilde{\lambda} \tilde{Q}_i^{(8)}(x)$$

$$\gamma = \gamma^{(0)} + \eta \gamma^{(6)} + \lambda \gamma^{(8)} + \tilde{\lambda} \tilde{\gamma}^{(8)}$$

- Second-order equations yield two families of solutions:

$$\gamma_+^{(0)}(\ell) = \ell \quad \text{with} \quad \ell \in \mathbb{N} \geq 2$$

$$\gamma_-^{(0)}(\ell) = \ell + 1 \quad \text{with} \quad \ell \in \mathbb{N} \geq 1$$

- Integer scaling dimensions ≥ 2 correspond to smooth horizons. For example, we can compute the Weyl curvature in ingoing Bondi-Sachs coordinates:

$$ds^2 = 2J\Omega^2 [-\rho^2 dv^2 + 2dv d\rho + h_{ab}(dy^a + U^a dv)(dy^b + U^b dv)]$$

Mapping to our other coordinates, we have:

$$C_{\rho a \rho b} = J (1 - \gamma) \rho^{\gamma-2} \varepsilon \left[\begin{array}{cc} -\frac{\gamma \Gamma_{\text{NH}}^2 (Q_1 + 2Q_2) \Omega_{\text{NH}}^2}{2(1-x^2)} & B_{\text{NH}}^2 \Omega_{\text{NH}}^2 Q'_4 \\ B_{\text{NH}}^2 \Omega_{\text{NH}}^2 Q'_4 & -\frac{\gamma B_{\text{NH}}^2 (Q_1 + 2Q_2) \Omega_{\text{NH}}^2}{2} \end{array} \right]$$

Perturbing the NHEK geometry

- Expand in Wilson coefficients:

$$Q_i(x) = Q_i^{(0)}(x) + \eta Q_i^{(6)}(x) + \lambda Q_i^{(8)}(x) + \tilde{\lambda} \tilde{Q}_i^{(8)}(x)$$
$$\gamma = \gamma^{(0)} + \eta \gamma^{(6)} + \lambda \gamma^{(8)} + \tilde{\lambda} \tilde{\gamma}^{(8)}$$

- Second-order equations yield two families of solutions:

$$\gamma_+^{(0)}(\ell) = \ell \quad \text{with} \quad \ell \in \mathbb{N} \geq 2$$
$$\gamma_-^{(0)}(\ell) = \ell + 1 \quad \text{with} \quad \ell \in \mathbb{N} \geq 1$$

- Integer scaling dimensions ≥ 2 correspond to smooth horizons. For example, we can compute the Weyl curvature in ingoing Bondi-Sachs coordinates:

$$ds^2 = 2J\Omega^2 \left[-\rho^2 dv^2 + 2dv d\rho + h_{ab}(dy^a + U^a dv)(dy^b + U^b dv) \right]$$

Away from extremality, $C \propto \rho^{\gamma-2} \implies C \propto T^{\gamma-2}$

Perturbing the EFT-corrected NHEK geometry

- EFT corrections to the $Q_i(x)$ functions can be obtained (too long to give here).

Perturbing the EFT-corrected NHEK geometry

- EFT corrections to the $Q_i(x)$ functions can be obtained (too long to give here).
- Important results are the corrections to the scaling dimensions. For example,

$$\gamma_+^{(6)}(2) = +\frac{24 \kappa^4}{7J^2}$$

$$\gamma_-^{(6)}(1) = +\frac{24 \kappa^4}{7J^2}$$

$$\gamma_+^{(8)}(2) = -\frac{21(32 + 45\pi)\kappa^6}{5J^3}$$

$$\gamma_-^{(8)}(1) = -\frac{9(8576 + 3045\pi)\kappa^6}{20J^3}$$

$$\tilde{\gamma}_+^{(8)}(2) = -\frac{12(736 + 315\pi)\kappa^6}{5J^3}$$

$$\tilde{\gamma}_-^{(8)}(1) = -\frac{189(384 + 145\pi)\kappa^6}{5J^3}$$

Perturbing the EFT-corrected NHEK geometry

- EFT corrections to the $Q_i(x)$ functions can be obtained (too long to give here).
- Important results are the corrections to the scaling dimensions. For example,

$$\gamma_+^{(6)}(2) = +\frac{24 \kappa^4}{7J^2}$$

$$\gamma_-^{(6)}(1) = +\frac{24 \kappa^4}{7J^2}$$

$$\gamma_+^{(8)}(2) = -\frac{21(32 + 45\pi)\kappa^6}{5J^3}$$

$$\gamma_-^{(8)}(1) = -\frac{9(8576 + 3045\pi)\kappa^6}{20J^3}$$

$$\tilde{\gamma}_+^{(8)}(2) = -\frac{12(736 + 315\pi)\kappa^6}{5J^3}$$

$$\tilde{\gamma}_-^{(8)}(1) = -\frac{189(384 + 145\pi)\kappa^6}{5J^3}$$

If $\eta < 0$ or $\lambda, \tilde{\lambda} > 0$, the *horizons* of extremal Kerr black holes will be singular.

Signs of couplings?

- We might think that this singularity *forbids* the couplings from achieving the sign that induces a singularity.

Signs of couplings?

- We might think that this singularity *forbids* the couplings from achieving the sign that induces a singularity.
- After all, certain signs of couplings violate infrared physics principles:
 - Causality of signal propagation
 - Analytic dispersion relations (locality and unitarity)

Adams et al. [hep-th/0602178]

Signs of couplings?

- We might think that this singularity *forbids* the couplings from achieving the sign that induces a singularity.
- After all, certain signs of couplings violate infrared physics principles:
 - Causality of signal propagation Adams et al. [hep-th/0602178]
 - Analytic dispersion relations (locality and unitarity)
- Examples:
 - Einstein-Maxwell theory Cheung, GR [1407.7865]; Cheung, Liu, GR [1801.08546, 1903.09156]
 - Higher-curvature gravity (R^2, R^4 terms) Bellazzini, Cheung, GR [1509.00851]; Cheung, GR [1608.02942]
 - Massive gravity Cheung, GR [1601.04068]
 - $(\partial\phi)^4$ and F^4 couplings Arkani-Hamed, Huang, Liu, GR [2109.13937]
 - Higher-point couplings Chandrasekaran, GR, Shahbazi-Moghaddam [1804.03153]; Arkani-Hamed, Cheung, Figueiredo, GR [2312.07652]
 - Cosmic inflation Kumar, Freytsis, GR, Rodd [2210.10791]
 - SMEFT GR, Rodd [1908.09845, 2004.02885, 2010.04723, 2206.13524]

Signs of couplings?

- We might think that this singularity *forbids* the couplings from achieving the sign that induces a singularity.
- After all, certain signs of couplings violate infrared physics principles:
 - Causality of signal propagation
 - Analytic dispersion relations (locality and unitarity)
- But **precisely the opposite holds:**
 - Causality and unitarity imply that $\lambda, \tilde{\lambda} > 0$

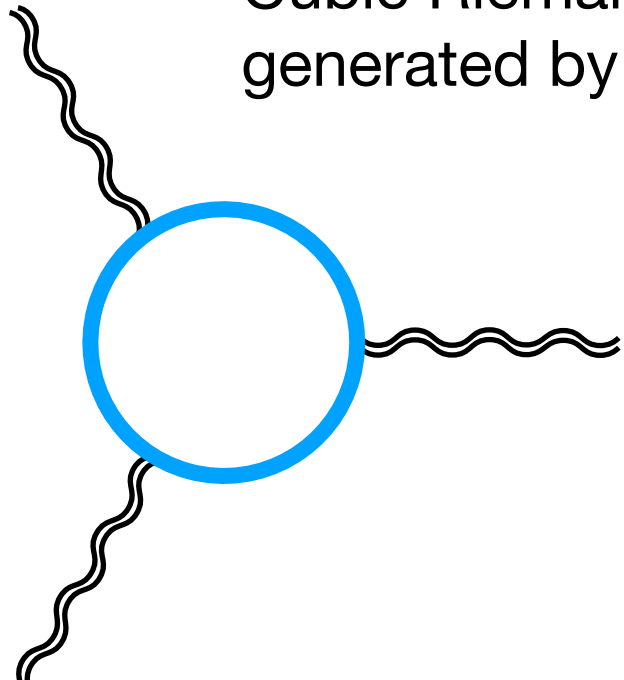
Bellazzini, Cheung, **GR** [1509.00851];
Gruzinov, Kleban [hep-th/0612015]

$$(\lambda, 4\tilde{\lambda}) = \frac{\alpha'^3}{256\kappa^6} \times \left\{ \begin{array}{lll} \left(13 + \zeta(3), 1 + \zeta(3) \right), & \left(\zeta(3), \zeta(3) \right), & \left(\frac{1}{2} + \zeta(3), \frac{1}{2} + \zeta(3) \right) \\ \text{bosonic} & \text{type II} & \text{type I / heterotic} \end{array} \right\}$$

- Quartic Riemann terms induce singularities.

Signs of couplings?

- We might think that this singularity *forbids* the couplings from achieving the sign that induces a singularity.
- After all, certain signs of couplings violate infrared physics principles:
 - Causality of signal propagation
 - Analytic dispersion relations (locality and unitarity)
- But **precisely the opposite holds:**
 - Cubic Riemann operator can take either sign. A threshold correction is generated by integrating out massive matter at one loop:

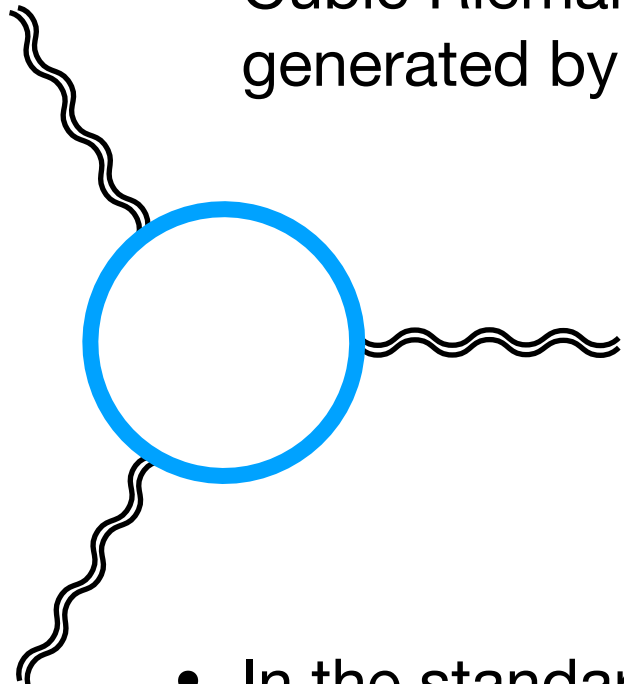


$$\eta = \frac{1}{15120(4\pi)^2 \kappa^2} \sum \left(\frac{1}{m_s^2} - \frac{4}{m_f^2} + \frac{3}{m_v^2} \right)$$

Adams et al. [hep-th/0602178]

Signs of couplings?

- We might think that this singularity *forbids* the couplings from achieving the sign that induces a singularity.
- After all, certain signs of couplings violate infrared physics principles:
 - Causality of signal propagation
 - Analytic dispersion relations (locality and unitarity)
- But **precisely the opposite holds:**
 - Cubic Riemann operator can take either sign. A threshold correction is generated by integrating out massive matter at one loop:



$$\eta = \frac{1}{15120(4\pi)^2 \kappa^2} \sum \left(\frac{1}{m_s^2} - \frac{4}{m_f^2} + \frac{3}{m_v^2} \right)$$

- In the standard model, the neutrinos are the lightest massive state, and $\eta < 0$.

⇒ singular horizons for extremal Kerr or new ultralight hidden-sector bosons

Adams et al. [hep-th/0602178]



Adding charge.

Adding a photon

- Let us now add a U(1) gauge field.
- Good reasons for doing this: first higher-derivative terms show up at fourth order in derivatives, rather than sixth \implies much larger effects

Adding a photon

- Let us now add a U(1) gauge field.
- Good reasons for doing this: first higher-derivative terms show up at fourth order in derivatives, rather than sixth \Rightarrow much larger effects
- Mode with $\gamma = 1$ will be physical for charged black holes. Defining the vectors

$$\ell = \partial/\partial\rho$$

$$m = \partial/\partial\phi$$

we will find the Weyl tensor near the horizon goes like

$$C_{abcd}\ell^a m^b \ell^c m^d \sim \gamma(\gamma - 1)\rho^{\gamma-2}$$

so there is a mode for which $C_{abcd}\ell^a m^b \ell^c m^d|_H \sim \delta\gamma/T$

- We will not need to be exponentially close to extremality to see the effect.

Einstein-Maxwell EFT

- Leading (four-derivative) contributions to the Einstein-Maxwell EFT:

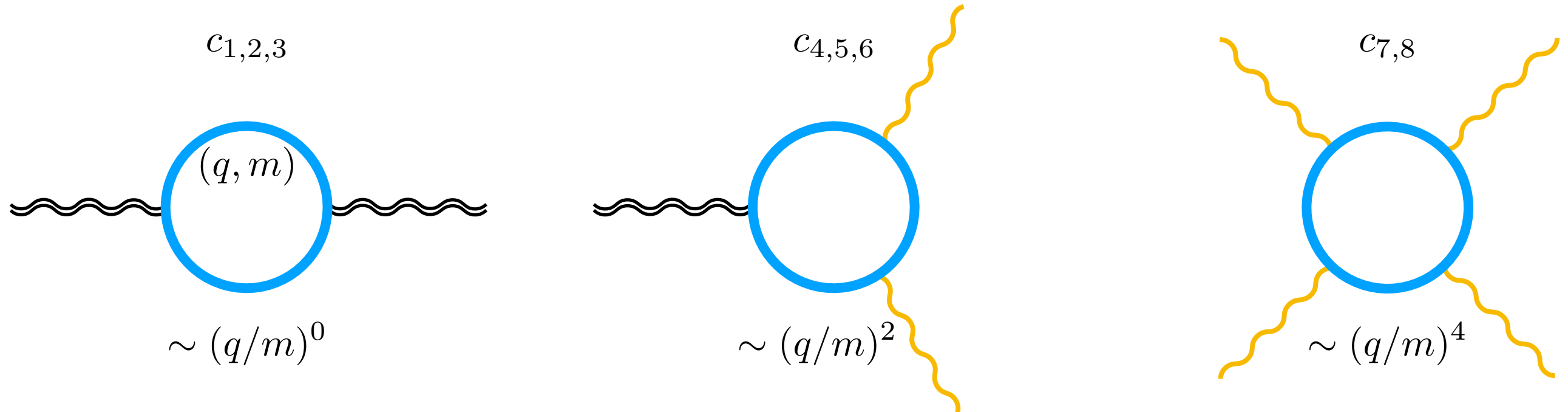
$$\begin{aligned}\mathcal{L} = & \frac{1}{2\kappa^2} R - \frac{1}{4} F_{ab} F^{ab} + c_1 R^2 + c_2 R^{ab} R_{ab} + c_3 R_{abcd} R^{abcd} \\ & + c_4 R F^{ab} F_{ab} + c_5 R^{ab} F_a{}^c F_{bc} + c_6 R^{abcd} F_{ab} F_{cd} \\ & + c_7 F_{ab} F^{ab} F_{cd} F^{cd} + c_8 F_{ab} F^{bc} F_{cd} F^{da}\end{aligned}$$

Einstein-Maxwell EFT

- Leading (four-derivative) contributions to the Einstein-Maxwell EFT:

$$\begin{aligned}\mathcal{L} = & \frac{1}{2\kappa^2}R - \frac{1}{4}F_{ab}F^{ab} + c_1 R^2 + c_2 R^{ab}R_{ab} + c_3 R_{abcd}R^{abcd} \\ & + c_4 RF^{ab}F_{ab} + c_5 R^{ab}F_a{}^c F_{bc} + c_6 R^{abcd}F_{ab}F_{cd} \\ & + c_7 F_{ab}F^{ab}F_{cd}F^{cd} + c_8 F_{ab}F^{bc}F_{cd}F^{da}\end{aligned}$$

Gravitational generalization of Euler-Heisenberg:



Convenient to rescale, so that $d_i \sim 1/\Lambda_{\text{UV}}^2$:

$$d_{1,2,3} = \kappa^2 c_{1,2,3}$$

$$d_{4,5,6} = c_{4,5,6}$$

$$d_{7,8} = \kappa^{-2} c_{7,8}$$

Einstein-Maxwell EFT

- Leading (four-derivative) contributions to the Einstein-Maxwell EFT:

$$\begin{aligned}\mathcal{L} = \frac{1}{2\kappa^2}R - \frac{1}{4}F_{ab}F^{ab} + c_1 R^2 + c_2 R^{ab}R_{ab} + c_3 R_{abcd}R^{abcd} \\ + c_4 RF^{ab}F_{ab} + c_5 R^{ab}F_a{}^c F_{bc} + c_6 R^{abcd}F_{ab}F_{cd} \\ + c_7 F_{ab}F^{ab}F_{cd}F^{cd} + c_8 F_{ab}F^{bc}F_{cd}F^{da}\end{aligned}$$

Under field redefinitions, only four combinations are invariant:

$$\left\{ \begin{array}{l} d_0 = d_2 + 4d_3 + d_5 + d_6 + 4d_7 + 2d_8 \\ d_3 \\ d_6 \\ d_9 = d_2 + 4d_3 + d_5 + 2d_6 + d_8 \end{array} \right.$$

Equivalently, since we can drop Gauss-Bonnet in $D = 4$, we can take $d_{6,7,8}$ as an operator basis.

EFT-corrected Einstein-Maxwell equations

- We wish to solve the EFT-corrected equations of motion:

$$\nabla^a F_{ab} = c_4 J_b^{c_4} + c_5 J_b^{c_5} + c_6 J_b^{c_6} + c_7 J_b^{c_7} + c_8 J_b^{c_8}$$

$$R_{ab} - \frac{1}{2} R g_{ab} - \kappa^2 \left(F_a{}^c F_{bc} - \frac{1}{4} g_{ab} F_{cd} F^{cd} \right) = \kappa^2 (c_1 T_{ab}^{c_1} + c_2 T_{ab}^{c_2} + c_3 T_{ab}^{c_3} + c_4 T_{ab}^{c_4} + c_5 T_{ab}^{c_5} + c_6 T_{ab}^{c_6} + c_7 T_{ab}^{c_7} + c_8 T_{ab}^{c_8})$$

$$J_a^{c_4} = 4(R\nabla^b F_{ba} - F_{ab}\nabla^b R)$$

$$J_a^{c_5} = -2(R_a{}^c \nabla_b F_c{}^b + R^{cb} \nabla_b F_{ac} + F_a{}^c \nabla_b R_c{}^b + F^{cb} \nabla_b R_{ac})$$

$$J_a^{c_6} = -4R_{adbc} \nabla^d F^{bc} - 4F^{bc} \nabla^d R_{adbc}$$

$$J_a^{c_7} = 8\nabla^e (F_{ea} F^{cd} F_{cd})$$

$$J_a^{c_8} = -8\nabla^b (F_a{}^p F_{cp} F_b{}^c)$$

$$T_{ab}^{c_1} = 4\nabla_a \nabla_b R - 4g_{ab} \square R - 4R_{ab} R + g_{ab} R^2$$

$$T_{ab}^{c_2} = 4\nabla_c \nabla_{(a} R_{b)}{}^c - 2\square R_{ab} - 2g_{ab} \nabla_d \nabla_c R^{cd} - 4R_a{}^c R_{bc} + g_{ab} R_{cd} R^{cd}$$

$$T_{ab}^{c_3} = -\left(4R_a{}^{cde} R_{bcde} - g_{ab} R_{cdef} R^{cdef} + 8\nabla_c \nabla_d R_{(a}{}^c{}_{b)}{}^d \right)$$

$$T_{ab}^{c_4} = 4F^{cd} \nabla_{(a} \nabla_{b)} F_{cd} + 4\nabla_a F^{cd} \nabla_b F_{cd} - 4g_{ab} F^{cd} \square F_{cd}$$

$$- 4g_{ab} \nabla_e F_{cd} \nabla^e F^{cd} - 2R_{ab} F_{cd} F^{cd} - 4F_a{}^c F_{bc} R + g_{ab} F_{cd} F^{cd} R$$

$$T_{ab}^{c_5} = 4F_{(a}{}^c R_{b)d} F_c{}^d - 2F_a{}^c F_b{}^d R_{cd} + g_{ab} F_c{}^e F^{cd} R_{de} - 2\nabla_{(a} F_{b)}{}^c \nabla_d F_c{}^d$$

$$- 2\nabla_d \nabla_{(a} F_{b)c} F^{cd} - 2\nabla_d \nabla_{(a} F^{cd} F_{b)c} - 2\square F_{(a}{}^c F_{b)c}$$

$$- g_{ab} F^{cd} \nabla_d \nabla^e F_{ce} - 2\nabla^d F_{(a}{}^c \nabla_{b)} F_{cd} - 2\nabla^d F_a{}^c \nabla_d F_{bc}$$

$$+ g_{ab} \nabla_c F^{cd} \nabla_e F_d{}^e - g_{ab} F^{cd} \nabla_e \nabla_d F_c{}^e - g_{ab} \nabla_d F_{ce} \nabla^e F^{cd}$$

$$T_{ab}^{c_6} = -\left(6F_{(a}{}^c F^{de} R_{b)cde} - g_{ab} F^{cd} F^{ef} R_{cdef} - 4F_{c(a} \nabla^c \nabla^d F_{b)d} \right.$$

$$\left. - 4F_{d(a} \nabla^d \nabla^c F_{b)d} + 4\nabla_c F_a{}^c \nabla_d F_b{}^d + 4\nabla_c F_{bd} \nabla^d F_a{}^c \right)$$

$$T_{ab}^{c_7} = F^{pq} F_{pq} (g_{ab} F^{cd} F_{cd} - 8F_{ac} F_b{}^c)$$

$$T_{ab}^{c_8} = g_{ab} F_c{}^p F_{dp} F^{cq} F_q{}^d - 8F_a{}^p F_{cp} F_b{}^q F_q{}^c$$

Kerr-Newman solution

- The solution to the Einstein-Maxwell equations for a charged, rotating black hole was found via an inspired guess by Ezra Newman in 1965: a complex coordinate transformation of Reissner-Nordström.

$$\begin{aligned} ds_{\text{KN}}^2 &= - \frac{\Delta(r)}{\Sigma(r, \theta)} (dt - a \sin^2 \theta d\phi)^2 + \Sigma(r, \theta) \left(\frac{dr^2}{\Delta(r)} + d\theta^2 \right) \\ &\quad + \frac{\sin^2 \theta}{\Sigma(r, \theta)} [a dt - (r^2 + a^2)d\phi]^2 \\ A_{\text{KN}} &= - \frac{\sqrt{2} Q r}{\kappa \Sigma(r, \theta)} (dt - a \sin^2 \theta d\phi) - \frac{\sqrt{2} P \cos \theta}{\kappa \Sigma(r, \theta)} [a dt - (r^2 + a^2)d\phi] \\ \Sigma(r, \theta) &= r^2 + a^2 \cos^2 \theta \\ \Delta(r) &= r^2 + a^2 - 2 M r + Q^2 + P^2 \end{aligned}$$

Kerr-Newman solution

- The solution to the Einstein-Maxwell equations for a charged, rotating black hole was found via an inspired guess by Ezra Newman in 1965: a complex coordinate transformation of Reissner-Nordström.

$$\begin{aligned} ds_{\text{KN}}^2 &= - \frac{\Delta(r)}{\Sigma(r, \theta)} (dt - a \sin^2 \theta d\phi)^2 + \Sigma(r, \theta) \left(\frac{dr^2}{\Delta(r)} + d\theta^2 \right) \\ &\quad + \frac{\sin^2 \theta}{\Sigma(r, \theta)} [a dt - (r^2 + a^2)d\phi]^2 \\ A_{\text{KN}} &= - \frac{\sqrt{2} Q r}{\kappa \Sigma(r, \theta)} (dt - a \sin^2 \theta d\phi) - \frac{\sqrt{2} P \cos \theta}{\kappa \Sigma(r, \theta)} [a dt - (r^2 + a^2)d\phi] \\ \Sigma(r, \theta) &= r^2 + a^2 \cos^2 \theta \\ \Delta(r) &= r^2 + a^2 - 2 M r + Q^2 + P^2 \end{aligned}$$

- Komar charges:

$$\begin{aligned} Q_e &= \lim_{r \rightarrow +\infty} \int_{S_r^2} \star F = \frac{4\pi\sqrt{2}}{\kappa} Q, & J &= \frac{1}{2\kappa^2} \lim_{r \rightarrow +\infty} \int_{S_r^2} \star dm = aE, \\ Q_m &= \lim_{r \rightarrow +\infty} \int_{S_r^2} F = \frac{4\pi\sqrt{2}}{\kappa} P, & E &= -\frac{1}{\kappa^2} \lim_{r \rightarrow +\infty} \int_{S_r^2} \star dk = \frac{8\pi M}{\kappa^2} \end{aligned}$$

Kerr-Newman solution

- Horizon: $r_+ = M + \sqrt{M^2 - a^2 - Q^2}$ generated by Killing vector $K = k + \Omega m$

Kerr-Newman solution

- Horizon: $r_+ = M + \sqrt{M^2 - a^2 - Q^2}$ generated by Killing vector $K = k + \Omega m$

- Angular velocity: $\Omega = \frac{a}{a^2 + r_+^2}$

- Temperature:

$$T = \frac{1}{2\pi} \sqrt{-\frac{1}{4} \left. \frac{\nabla_a (K^c K_c) \nabla^a (K^d K_d)}{K^e K_e} \right|_H} = \frac{r_+^2 - a^2 - Q^2}{4\pi r_+ (r_+^2 + a^2)}$$

- Chemical potential:

$$\mu = -\frac{\kappa}{\sqrt{2}} \left(K^a A_a|_H - \lim_{r \rightarrow +\infty} K^a A_a \right) = \frac{Q}{r_+^2 + a^2}$$

Kerr-Newman solution

- Horizon: $r_+ = M + \sqrt{M^2 - a^2 - Q^2}$ generated by Killing vector $K = k + \Omega m$

- Angular velocity: $\Omega = \frac{a}{a^2 + r_+^2}$

- Temperature:

$$T = \frac{1}{2\pi} \sqrt{-\frac{1}{4} \left. \frac{\nabla_a(K^c K_c) \nabla^a(K^d K_d)}{K^e K_e} \right|_H} = \frac{r_+^2 - a^2 - Q^2}{4\pi r_+ (r_+^2 + a^2)}$$

- Chemical potential:

$$\mu = -\frac{\kappa}{\sqrt{2}} \left(K^a A_a|_H - \lim_{r \rightarrow +\infty} K^a A_a \right) = \frac{Q}{r_+^2 + a^2}$$

- Entropy:

$$S_W = -2\pi \oint_{\mathcal{B}^+} d^2x \sqrt{\sigma} \frac{\delta \mathcal{L}}{\delta R_{abcd}} \varepsilon_{ab} \varepsilon_{cd}$$

$$S_{\text{BH}} = \lim_{c_i \rightarrow 0} S_W = \frac{2\pi A}{\kappa^2}$$

- First law of black hole mechanics: $dM = T dS_W + \mu dQ + \Omega dJ$

Near-horizon geometry

- Like the NHEK for Kerr, the Kerr-Newman solution enjoys an $O(2, 1) \times U(1)$ symmetric near-horizon geometry, discovered fairly recently:

Hartman, Murata, Nishioka, Strominger [0811.4393]

$$\begin{aligned} ds_{\text{NH-KN}}^2 &= 2M^2[F_1^{(0)}(x)]^2 \left[-\rho^2 d\tau^2 + \frac{d\rho^2}{\rho^2} + \frac{dx^2}{1-x^2} \right. \\ &\quad \left. + [F_2^{(0)}(x)]^2(1-x^2) \left(d\varphi + \rho \omega_{\text{NH}}^{(0)} d\tau \right)^2 \right] \\ A_{\text{NH-KN}} &= \frac{\sqrt{2} M}{\kappa} \left[Q_{\text{NH}}^{(0)} \rho d\tau + (1-x^2) F_2^{(0)}(x) F_3^{(0)}(x) \left(d\varphi + \rho \omega_{\text{NH}}^{(0)} d\tau \right) \right] \end{aligned}$$

$$\begin{aligned} F_1^{(0)}(x) &= \frac{\sqrt{1+(1-Z^2)x^2}}{\sqrt{2}}, & F_2^{(0)}(x) &= \frac{(2-Z^2)}{1+(1-Z^2)x^2}, & F_3^{(0)}(x) &= \frac{Z\sqrt{1-Z^2}}{2-Z^2}, \\ \omega_{\text{NH}}^{(0)} &= \frac{2\sqrt{1-Z^2}}{2-Z^2}, & \text{and} & \quad Q_{\text{NH}}^{(0)} = \frac{Z^3}{2-Z^2} & & Z = Q/M \end{aligned}$$

Connecting to asymptotia

- As in the Kerr case, the modes solving the linearized equations in the near-horizon background give us the first corrections connecting this solution to full Kerr-Newman. We start with the ansatz:

$$\begin{aligned} ds^2 = 2M^2 [f_1^{(0)}(x, \rho)]^2 & \left[-\rho^2 d\tau^2 + \frac{d\rho^2}{\rho^2} + \frac{dx^2}{f_6^{(0)}(x, \rho) (1 - x^2)} \right. \\ & \left. + f_2^{(0)}(x, \rho)^2 (1 - x^2) \left(d\varphi + \rho f_4^{(0)}(x, \rho) d\tau \right)^2 \right] \end{aligned}$$

Connecting to asymptotia

- As in the Kerr case, the modes solving the linearized equations in the near-horizon background give us the first corrections connecting this solution to full Kerr-Newman. We start with the ansatz:

$$\begin{aligned} ds^2 = 2M^2 [f_1^{(0)}(x, \rho)]^2 & \left[-\rho^2 d\tau^2 + \frac{d\rho^2}{\rho^2} + \frac{dx^2}{f_6^{(0)}(x, \rho) (1 - x^2)} \right. \\ & \left. + f_2^{(0)}(x, \rho)^2 (1 - x^2) \left(d\varphi + \rho f_4^{(0)}(x, \rho) d\tau \right)^2 \right] \end{aligned}$$

- Modes:

$$f_i^{(0)}(x, \rho) = F_i^{(0)}(x) \left[1 + \delta \hat{f}_i^{(0)}(x, \rho) \right] \quad \text{for } i = 1, 2, 3$$

$$f_4^{(0)}(x, \rho) = \omega_{\text{NH}}^{(0)} \left[1 + \delta \hat{f}_4^{(0)}(x, \rho) \right]$$

$$f_5^{(0)}(x, \rho) = Q_{\text{NH}}^{(0)} \left[1 + \delta \hat{f}_5^{(0)}(x, \rho) \right]$$

$$f_6^{(0)}(x, \rho) = 1 + \delta \hat{f}_6^{(0)}(x, \rho)$$

$$\delta \hat{f}_i^{(0)}(x, \rho) = \rho^{\gamma^{(0)}} \delta f_i^{(0)}(x)$$

O(2, 1) harmonics, for $\gamma^{(0)} \neq 1$

Connecting to asymptotia

- We expect four physical modes: two for the graviton and two for the photon. But since we are in a background with nonzero electric field, the photon and graviton kinetically mix. To disentangle them, we make the substitution:

$$\delta f_1^{(0)}(x) = \frac{v_1(x)}{2} + \frac{1}{1 + (1 - Z^2)x^2} \left[\frac{Z^2(1 - x^2)}{2 + Z^2} v_4(x) - (2 - Z^2)x(1 - x^2) \frac{v'_1(x)}{4} \right. \\ \left. + (2 + Z^2)(1 - Z^2)(1 - x^2)^2 \frac{v'_2(x)}{x} - Z^4(2 + Z^2)(1 - Z^2)x(1 - x^2)v'_3(x) \right]$$

$$\delta f_2^{(0)}(x) = -\frac{v_1(x)}{2} - \frac{2}{1 + (1 - Z^2)x^2} \left[\frac{Z^2(1 - x^2)}{2 + Z^2} v_4(x) - (2 - Z^2)x(1 - x^2) \frac{v'_1(x)}{4} \right. \\ \left. + (2 + Z^2)(1 - Z^2)(1 - x^2)^2 \frac{v'_2(x)}{x} - Z^4(2 + Z^2)(1 - Z^2)x(1 - x^2)v'_3(x) \right]$$

$$\delta f_3^{(0)}(x) = \frac{v_1(x)}{2} + v_4(x) - Z^2(2 + Z^2)(1 - x^2) \frac{v'_2(x)}{x} - Z^2(2 + Z^2)(2 - 3Z^2)xv'_3(x)$$

$$\delta f_4^{(0)}(x) = \frac{1}{\gamma^{(0)} + 1} \left[\frac{2(1 + x^2) + \lambda^{(0)}(1 - x^2)}{2} \frac{v_1(x)}{2} + \lambda^{(0)}(4 - Z^4)v_2(x) \right. \\ \left. + \lambda^{(0)}Z^4(2 + Z^2)v_3(x) + \frac{Z^2}{2 + Z^2}(1 + x^2)v_4(x) \right. \\ \left. - x(1 - x^2) \frac{v'_1(x)}{2} - \frac{Z^2}{2 + Z^2}x(1 - x^2)v'_4(x) \right]$$

$$\delta f_5^{(0)}(x) = \frac{1}{\gamma^{(0)} + 1} \left[\frac{2(1 + x^2) + \lambda^{(0)}(1 - x^2)}{2} \frac{v_1(x)}{2} - \lambda^{(0)}(2 + Z^2)^2(1 - Z^2)v_3(x) \right. \\ \left. - \frac{2 - 3Z^2}{2 + Z^2}(1 + x^2) \frac{v_4(x)}{Z^2} - x(1 - x^2) \frac{v'_1(x)}{2} \right. \\ \left. + \frac{2 - 3Z^2}{2 + Z^2}x(1 - x^2) \frac{v'_4(x)}{Z^2} \right]$$

$$\delta f_6^{(0)}(x) = v_1(x)$$

Connecting to asymptotia

- The Einstein-Maxwell equations then take the simple form:

$$[(1-x^2)^2 v'_1]' + [\gamma^{(0)}(\gamma^{(0)}+1) - 2](1-x^2)v_1 = 0$$

$$\left[\frac{(1-x^2)^2}{x^2} v'_2 \right]' + \gamma^{(0)}(\gamma^{(0)}+1) \frac{1-x^2}{x^2} v_2 = 0$$

$$[(1-x^2)v'_3]' + \gamma^{(0)}(\gamma^{(0)}+1)v_3 = 0$$

$$[(1-x^2)^2 v'_4]' + [\gamma^{(0)}(\gamma^{(0)}+1) - 2](1-x^2)v_4 = 0$$

Connecting to asymptotia

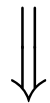
- The Einstein-Maxwell equations then take the simple form:

$$[(1-x^2)^2 v'_1]' + [\gamma^{(0)}(\gamma^{(0)}+1) - 2](1-x^2)v_1 = 0$$

$$\left[\frac{(1-x^2)^2}{x^2} v'_2 \right]' + \gamma^{(0)}(\gamma^{(0)}+1) \frac{1-x^2}{x^2} v_2 = 0$$

$$[(1-x^2)v'_3]' + \gamma^{(0)}(\gamma^{(0)}+1)v_3 = 0$$

$$[(1-x^2)^2 v'_4]' + [\gamma^{(0)}(\gamma^{(0)}+1) - 2](1-x^2)v_4 = 0$$



$$v_1(x) = P'_{\ell_1}(x), \quad \gamma_1^{(0)} = \ell_1$$

$$v_2(x) = x(\ell_2 + 1)\ell_2 P_{\ell_2}(x) + (1 + x^2\ell_2)P'_{\ell_2}(x), \quad \gamma_2^{(0)} = \ell_2 + 1$$

$$v_3(x) = P_{\ell_3}(x), \quad \gamma_3^{(0)} = \ell_3$$

$$v_4(x) = P'_{\ell_4}(x), \quad \gamma_4^{(0)} = \ell_4$$

$$\ell_{1,3,4} \geq 2, \quad \ell_2 \geq 1$$

Connecting to asymptotia

- The Einstein-Maxwell equations then take the simple form:

$$[(1-x^2)^2 v'_1]' + [\gamma^{(0)}(\gamma^{(0)}+1) - 2](1-x^2)v_1 = 0$$

$$\left[\frac{(1-x^2)^2}{x^2} v'_2 \right]' + \gamma^{(0)}(\gamma^{(0)}+1) \frac{1-x^2}{x^2} v_2 = 0$$

$$[(1-x^2)v'_3]' + \gamma^{(0)}(\gamma^{(0)}+1)v_3 = 0$$

$$[(1-x^2)^2 v'_4]' + [\gamma^{(0)}(\gamma^{(0)}+1) - 2](1-x^2)v_4 = 0$$



$$v_1(x) = P'_{\ell_1}(x),$$

$$\gamma_1^{(0)} = \ell_1$$

$$v_2(x) = x(\ell_2 + 1)\ell_2 P_{\ell_2}(x) + (1 + x^2\ell_2)P'_{\ell_2}(x),$$

$$\gamma_2^{(0)} = \ell_2 + 1$$

$$v_3(x) = P_{\ell_3}(x),$$

$$\gamma_3^{(0)} = \ell_3$$

$$v_4(x) = P'_{\ell_4}(x),$$

$$\gamma_4^{(0)} = \ell_4$$

axial: $(-1)^{\ell+1}$ under parity

$$\ell_{1,3,4} \geq 2, \quad \ell_2 \geq 1$$

Connecting to asymptotia

- The Einstein-Maxwell equations then take the simple form:

$$[(1-x^2)^2 v'_1]' + [\gamma^{(0)}(\gamma^{(0)}+1) - 2](1-x^2)v_1 = 0$$

$$\left[\frac{(1-x^2)^2}{x^2} v'_2 \right]' + \gamma^{(0)}(\gamma^{(0)}+1) \frac{1-x^2}{x^2} v_2 = 0$$

$$[(1-x^2)v'_3]' + \gamma^{(0)}(\gamma^{(0)}+1)v_3 = 0$$

$$[(1-x^2)^2 v'_4]' + [\gamma^{(0)}(\gamma^{(0)}+1) - 2](1-x^2)v_4 = 0$$



 $v_1(x) = P'_{\ell_1}(x),$

$$\gamma_1^{(0)} = \ell_1$$

 $v_2(x) = x(\ell_2 + 1)\ell_2 P_{\ell_2}(x) + (1 + x^2\ell_2)P'_{\ell_2}(x),$

$$\gamma_2^{(0)} = \ell_2 + 1$$

 $v_3(x) = P_{\ell_3}(x),$

$$\gamma_3^{(0)} = \ell_3$$

 $v_4(x) = P'_{\ell_4}(x),$

$$\gamma_4^{(0)} = \ell_4$$

axial: $(-1)^{\ell+1}$ under parity

$$\ell_{1,3,4} \geq 2, \quad \ell_2 \geq 1$$

polar: $(-1)^\ell$ under parity

Connecting to asymptotia

- For $\gamma^{(0)} = 1$, there are various complications: residual gauge symmetry, plus non-power law terms that we must include, shifting $\delta f_i^{(0)}$ by terms $\propto \rho$ and $\rho \log \rho$. These are coordinate artifacts and do not contribute to tidal force singularities.

Connecting to asymptotia

- For $\gamma^{(0)} = 1$, there are various complications: residual gauge symmetry, plus non-power law terms that we must include, shifting $\delta f_i^{(0)}$ by terms $\propto \rho$ and $\rho \log \rho$. These are coordinate artifacts and do not contribute to tidal force singularities.
- We will focus on the even-parity $\gamma^{(0)} = 1$ modes.

$$\begin{aligned}\ell_2 &= 0 \\ \implies \ell_1 &= 1 \\ \ell_4 &= 1\end{aligned}$$

Connecting to asymptotia

- For $\gamma^{(0)} = 1$, there are various complications: residual gauge symmetry, plus non-power law terms that we must include, shifting $\delta f_i^{(0)}$ by terms $\propto \rho$ and $\rho \log \rho$. These are coordinate artifacts and do not contribute to tidal force singularities.
- We will focus on the even-parity $\gamma^{(0)} = 1$ modes.

$$\begin{aligned} \ell_2 &= 0 \text{ vanishes identically} \\ \implies \ell_1 &= 1 \text{ pure gauge} \\ \ell_4 &= 1 \end{aligned}$$

EFT-correcting the near-horizon modes

- As always, choose an ansatz with the appropriate near-horizon symmetry:

$$ds_{\text{NH}}^2 = 2M^2 [F_1(x)]^2 \left[-\rho^2 d\tau^2 + \frac{d\rho^2}{\rho^2} + \frac{\Gamma_{\text{NH}}^2 dx^2}{1-x^2} + [F_2(x)]^2 (1-x^2) (d\varphi + \rho \omega_{\text{NH}} d\tau)^2 \right]$$

$$A_{\text{NH}} = \frac{\sqrt{2}M}{\kappa} [Q_{\text{NH}} \rho d\tau + (1-x^2) F_2(x) F_3(x) (d\varphi + \rho \omega_{\text{NH}} d\tau)]$$

$$F_i(x) = F_i^{(0)}(x) \left[1 + \sum_{K=1}^8 \frac{d_K}{M^2} \delta F_i^{(K)}(x) \right], \quad i = 1, 2, 3$$

$$\Gamma_{\text{NH}} = 1 + \sum_{K=1}^8 \frac{d_K}{M^2} \delta \Gamma_{\text{NH}}^{(K)}$$

$$\omega_{\text{NH}} = \omega_{\text{NH}}^{(0)} \left(1 + \sum_{K=1}^8 \frac{d_K}{M^2} \delta \omega_{\text{NH}}^{(K)} \right)$$

$$Q_{\text{NH}} = Q_{\text{NH}}^{(0)} \left(1 + \sum_{K=1}^8 \frac{d_K}{M^2} \delta Q_{\text{NH}}^{(K)} \right)$$

Analytically compute all quantities to first order in the Wilson coefficients.

EFT-correcting the near-horizon modes

- Compute linearized deformations *around* the EFT-corrected near-horizon background, and map onto our $O(2,1)$ modes defined previously.

EFT-correcting the near-horizon modes

- Compute linearized deformations *around* the EFT-corrected near-horizon background, and map onto our $O(2,1)$ modes defined previously.
- Generates corrections to scaling dimensions:

$$\mathfrak{a} = a/r_+ \in [0, 1]$$

$$\delta\gamma^{(1)} = \delta\gamma^{(4)} = 0$$

$$\delta\gamma^{(2)} = \delta\gamma^{(5)} = \frac{1}{4}\delta\gamma^{(3)}$$

$$\delta\gamma^{(5)} = 4\delta\gamma^{(8)} - \delta\gamma^{(7)}$$

$$\begin{aligned} \delta\gamma^{(6)} = & \frac{3(\mathfrak{a}^2 - 1)}{10\mathfrak{a}^4(\mathfrak{a}^2 + 1)^4} (15 + 25\mathfrak{a}^2 - 201\mathfrak{a}^4 + 89\mathfrak{a}^6 - 187\mathfrak{a}^8 + 195\mathfrak{a}^{10} + 245\mathfrak{a}^{12} + 75\mathfrak{a}^{14}) \\ & + \frac{9(\mathfrak{a}^2 - 1)^2(\mathfrak{a}^2 + 1)(1 - 2\mathfrak{a}^2 + 5\mathfrak{a}^4)}{2\mathfrak{a}^5} \arctan \mathfrak{a} \end{aligned}$$

$$\delta\gamma^{(7)} = \delta\gamma^{(6)} + \frac{16(\mathfrak{a}^2 - 1)}{5(\mathfrak{a}^2 + 1)^6} (149 - 522\mathfrak{a}^2 + 436\mathfrak{a}^4 - 166\mathfrak{a}^6 + 7\mathfrak{a}^8)$$

$$\delta\gamma^{(8)} = \frac{3}{4}\delta\gamma^{(6)} + \frac{4(\mathfrak{a}^2 - 1)}{5(\mathfrak{a}^2 + 1)^6} (167 - 558\mathfrak{a}^2 + 316\mathfrak{a}^4 - 226\mathfrak{a}^6 + 13\mathfrak{a}^8)$$

EFT-correcting the near-horizon modes

- Compute linearized deformations *around* the EFT-corrected near-horizon background, and map onto our $O(2,1)$ modes defined previously.
- Generates corrections to scaling dimensions: $\mathfrak{a} = a/r_+ \in [0, 1]$

$$\delta\gamma^{(1)} = \delta\gamma^{(4)} = 0$$

$$\delta\gamma^{(2)} = \delta\gamma^{(5)} = \frac{1}{4}\delta\gamma^{(3)}$$

$$\delta\gamma^{(5)} = 4\delta\gamma^{(8)} - \delta\gamma^{(7)}$$

$$\begin{aligned} \delta\gamma^{(6)} &= \frac{3(\mathfrak{a}^2 - 1)}{10\mathfrak{a}^4(\mathfrak{a}^2 + 1)^4} (15 + 25\mathfrak{a}^2 - 201\mathfrak{a}^4 + 89\mathfrak{a}^6 - 187\mathfrak{a}^8 + 195\mathfrak{a}^{10} + 245\mathfrak{a}^{12} + 75\mathfrak{a}^{14}) \\ &\quad + \frac{9(\mathfrak{a}^2 - 1)^2(\mathfrak{a}^2 + 1)(1 - 2\mathfrak{a}^2 + 5\mathfrak{a}^4)}{2\mathfrak{a}^5} \arctan \mathfrak{a} \end{aligned}$$

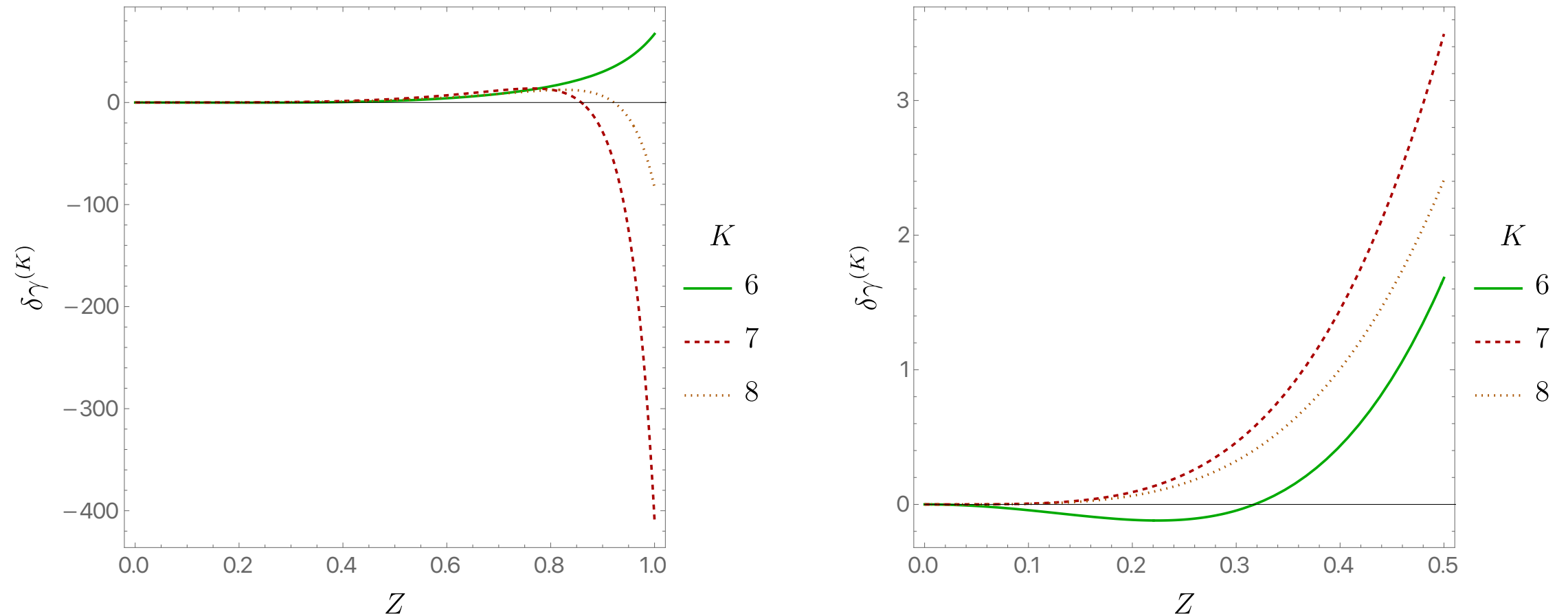
$$\delta\gamma^{(7)} = \delta\gamma^{(6)} + \frac{16(\mathfrak{a}^2 - 1)}{5(\mathfrak{a}^2 + 1)^6} (149 - 522\mathfrak{a}^2 + 436\mathfrak{a}^4 - 166\mathfrak{a}^6 + 7\mathfrak{a}^8)$$

$$\delta\gamma^{(8)} = \frac{3}{4}\delta\gamma^{(6)} + \frac{4(\mathfrak{a}^2 - 1)}{5(\mathfrak{a}^2 + 1)^6} (167 - 558\mathfrak{a}^2 + 316\mathfrak{a}^4 - 226\mathfrak{a}^6 + 13\mathfrak{a}^8)$$

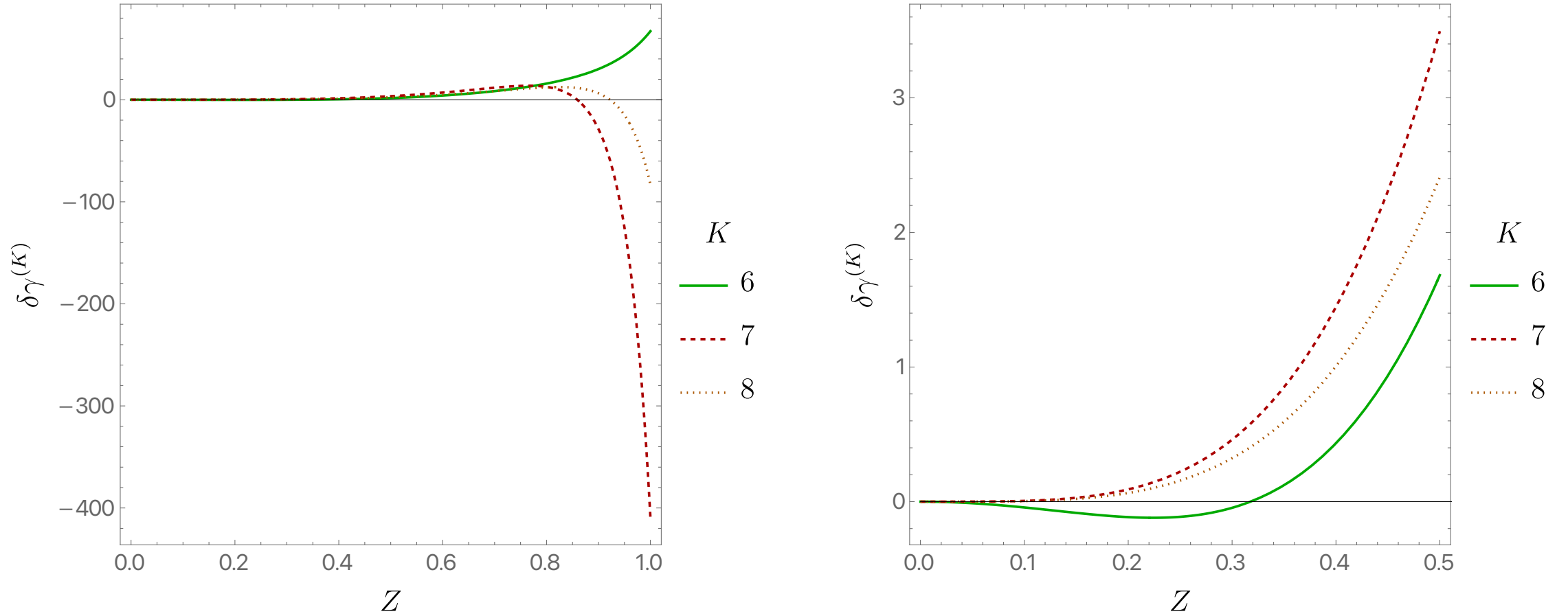
- Full shift is field redefinition invariant, representing a nontrivial check:

$$\sum_{K=1}^8 d_K \delta\gamma^{(K)} = \frac{1}{4}\delta\gamma^{(7)}d_0 + \left(\delta\gamma^{(6)} + \frac{3}{4}\delta\gamma^{(7)} - 2\delta\gamma^{(8)} \right) d_6 + \left(\delta\gamma^{(8)} - \frac{1}{2}\delta\gamma^{(7)} \right) d_9$$

EFT-correcting the near-horizon modes



EFT-correcting the near-horizon modes



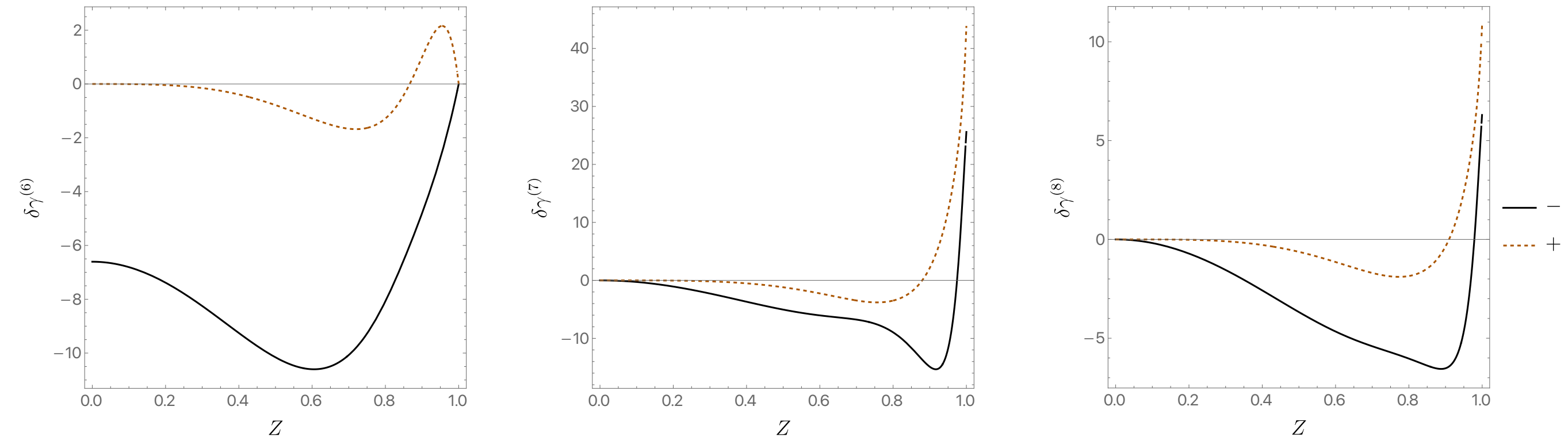
In ingoing Bondi-Sachs coordinates, we find a Weyl curvature singularity, irrespective of the sign of the Wilson coefficients:

$$C_{\rho a \rho b} = \frac{1 - Z^2}{4\rho} \begin{bmatrix} -\frac{1}{2 - Z^2} & -\frac{\sqrt{1 - Z^2} x}{1 + (1 - Z^2)x^2} \\ -\frac{\sqrt{1 - Z^2} x}{1 + (1 - Z^2)x^2} & \frac{(2 - Z^2)(1 - x^2)}{[1 + (1 - Z^2)x^2]^2} \end{bmatrix} \sum_{K=1}^8 d_K \delta\gamma^{(K)}$$

Power-law divergence, and vanishes for extreme, non-spinning Reissner-Nordström.

EFT-correcting the near-horizon modes

Correction to scaling dimension is generically nonzero. For example, the two even-parity $\gamma^{(0)} = 2$ modes:



Finite temperature

Away from extremality

- To explicitly compute EFT-corrected black holes *away from the extremal limit*, i.e., at finite temperature, we will need to solve the equations numerically.

$$\begin{aligned} ds^2 = & - \frac{\Delta(r)}{\Sigma(r, X)} F_1(r, X) [dt - (1 - X^2) F_4(r, X) d\phi]^2 \\ & + \frac{1 - X^2}{\Sigma(r, X)} F_3(r, X) [F_4(r, X) dt - (r^2 + a^2) d\phi]^2 \\ & + \Sigma(r, X) F_2(r, X) \left[\frac{dr^2}{\Delta(r)} + \frac{dX^2}{1 - X^2} \right] \\ A = & - \frac{\sqrt{2} r F_5(r, X)}{\kappa \Sigma(r, X)} [dt - F_4(r, X) (1 - X^2) d\phi] \\ & - \frac{\sqrt{2} (1 - X^2) F_6(r, X)}{\kappa \Sigma(r, X)} [F_4(r, X) dt - (r^2 + a^2) d\phi] \end{aligned}$$

$$\begin{aligned} F_i(r, X) &= 1 + \sum_{K=6}^8 \frac{d_K}{M^2} f_i^{(K)}(r, X), \quad i = 1, 2, 3 & F_5(r, X) &= \bar{Q} + \left(1 - \frac{r_+}{r}\right) \sum_{K=6}^8 \frac{d_K}{M^2} f_5^{(K)}(r, X) \\ F_4(r, X) &= \bar{a} + \left(1 - \frac{r_+}{r}\right) \sum_{K=6}^8 \frac{d_K}{M^2} f_4^{(K)}(r, X) & F_6(r, X) &= \sum_{K=6}^8 \frac{d_K}{M^2} f_6^{(K)}(r, X) \end{aligned}$$

Away from extremality

- To explicitly compute EFT-corrected black holes *away from the extremal limit*, i.e., at finite temperature, we will need to solve the equations numerically.
- We will numerically solve the EFT-corrected Einstein-Maxwell equations *away from the horizon* as well, out to $r = \infty$. Compactify coordinates using

$$r = \frac{r_+}{1 - Y}$$

$Y = 0$ horizon

$Y = 1$ infinity

- Due to large gradients near horizon, must use multiple Chebyshev-Gauss-Lobatto grids, and patch at interfaces.

Probing the horizon singularity

- Once we have constructed the solutions, we can measure the EFT-generated singularity at the horizon using an ingoing null geodesic: a massless probe falling into the horizon. Coordinates: $\dot{x} = (\dot{t}(\lambda), \dot{r}(\lambda), \dot{X}(\lambda), \dot{\phi}(\lambda))$

Probing the horizon singularity

- Once we have constructed the solutions, we can measure the EFT-generated singularity at the horizon using an ingoing null geodesic: a massless probe falling into the horizon. Coordinates: $\dot{x} = (\dot{t}(\lambda), \dot{r}(\lambda), \dot{X}(\lambda), \dot{\phi}(\lambda))$
- Choose geodesic in equatorial plane ($X = 0$), with zero angular momentum ($\partial(\dot{x}^2)/\partial\dot{\phi} = 0$), and write in ingoing Bondi-Sachs coordinates:

$$dt = dv - \frac{dr}{\Delta(r)} (r_+^2 + \bar{a}^2) \left(1 - \frac{1}{2r_+^2} \sum_{K=6}^8 \lambda^K d_K \right),$$

$$d\phi = d\varphi - \bar{a} \frac{dr}{\Delta(r)} \left(1 - \frac{1}{2r_+^2} \sum_{K=6}^8 \lambda^K d_K \right)$$

$$\dot{x} = \frac{r^2}{\Delta(r)f_1(r,0)f_3(r,0)[r^2 + \bar{a}^2 - f_4(r,0)^2]} \begin{bmatrix} \frac{(\bar{a}^2 + r^2)^2 f_3(r,0) - \Delta(r)f_1(r,0)f_4(r,0)^2}{\bar{a}^2 + r^2 - f_4(r,0)^2} \\ - \frac{\Delta(r)\sqrt{f_1(r,0)f_3(r,0)}\sqrt{(\bar{a}^2 + r^2)^2 f_3(r,0) - \Delta(r)f_1(r,0)f_4(r,0)^2}}{r^2 \sqrt{f_2(r,0)}} \\ 0 \\ \frac{(\bar{a}^2 + r^2)f_3(r,0) - \Delta(r)f_1(r,0)}{\bar{a}^2 + r^2 - f_4(r,0)^2} f_4(r,0) \end{bmatrix}$$

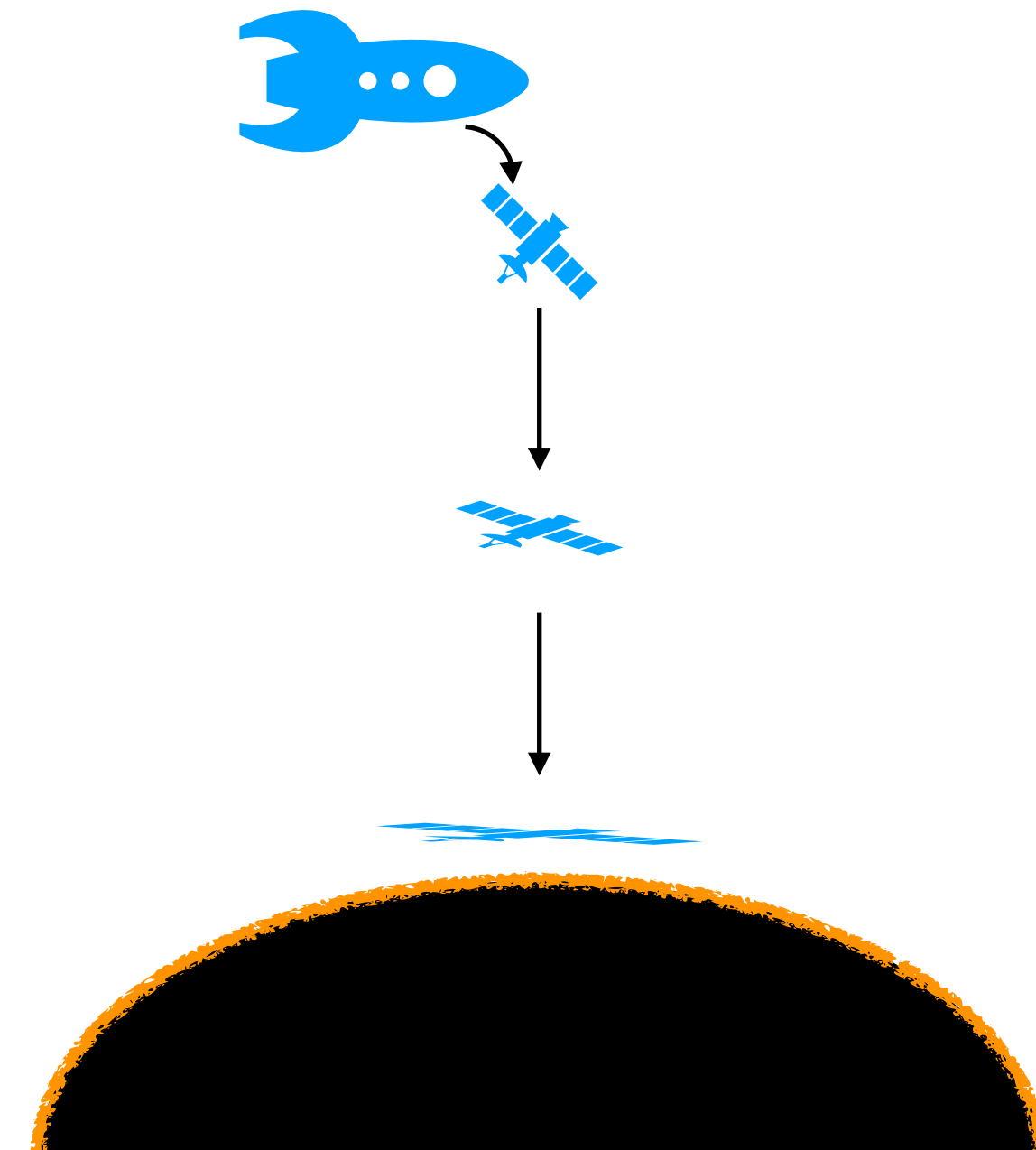
Probing the horizon singularity

- Once we have constructed the solutions, we can measure the EFT-generated singularity at the horizon using an ingoing null geodesic: a massless probe falling into the horizon. Coordinates: $\dot{x} = (\dot{t}(\lambda), \dot{r}(\lambda), \dot{X}(\lambda), \dot{\phi}(\lambda))$

- Define a tidal force observable:

$$C_{\varphi\varphi} = \dot{x}^a \dot{x}^b C_{\varphi a \varphi b}$$

- Measure on horizon at equator: $C_{\varphi\varphi}^{\mathcal{H}}$



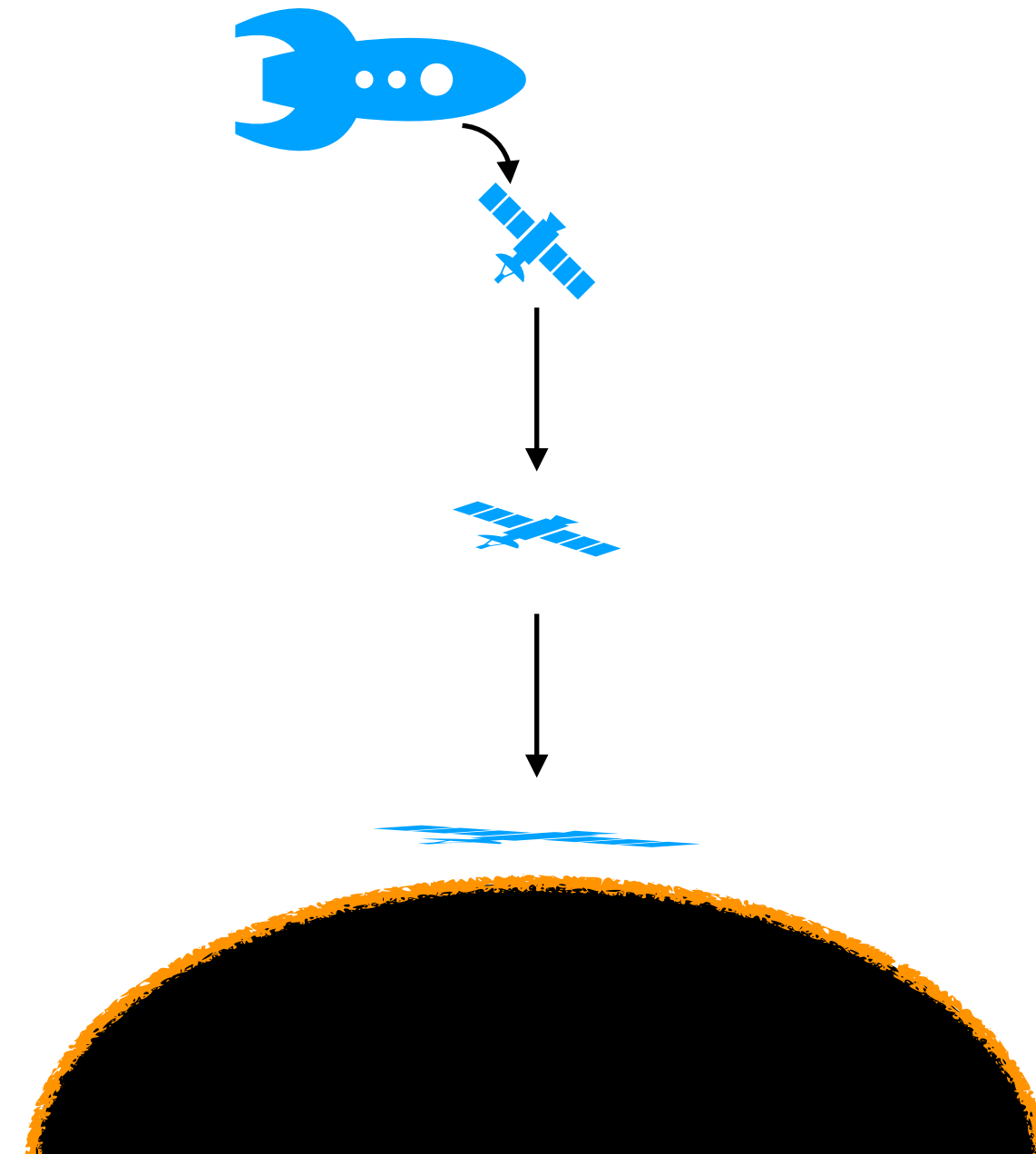
Probing the horizon singularity

- Once we have constructed the solutions, we can measure the EFT-generated singularity at the horizon using an ingoing null geodesic: a massless probe falling into the horizon. Coordinates: $\dot{x} = (\dot{t}(\lambda), \dot{r}(\lambda), \dot{X}(\lambda), \dot{\phi}(\lambda))$
- Define a tidal force observable:

$$C_{\varphi\varphi} = \dot{x}^a \dot{x}^b C_{\varphi a \varphi b}$$

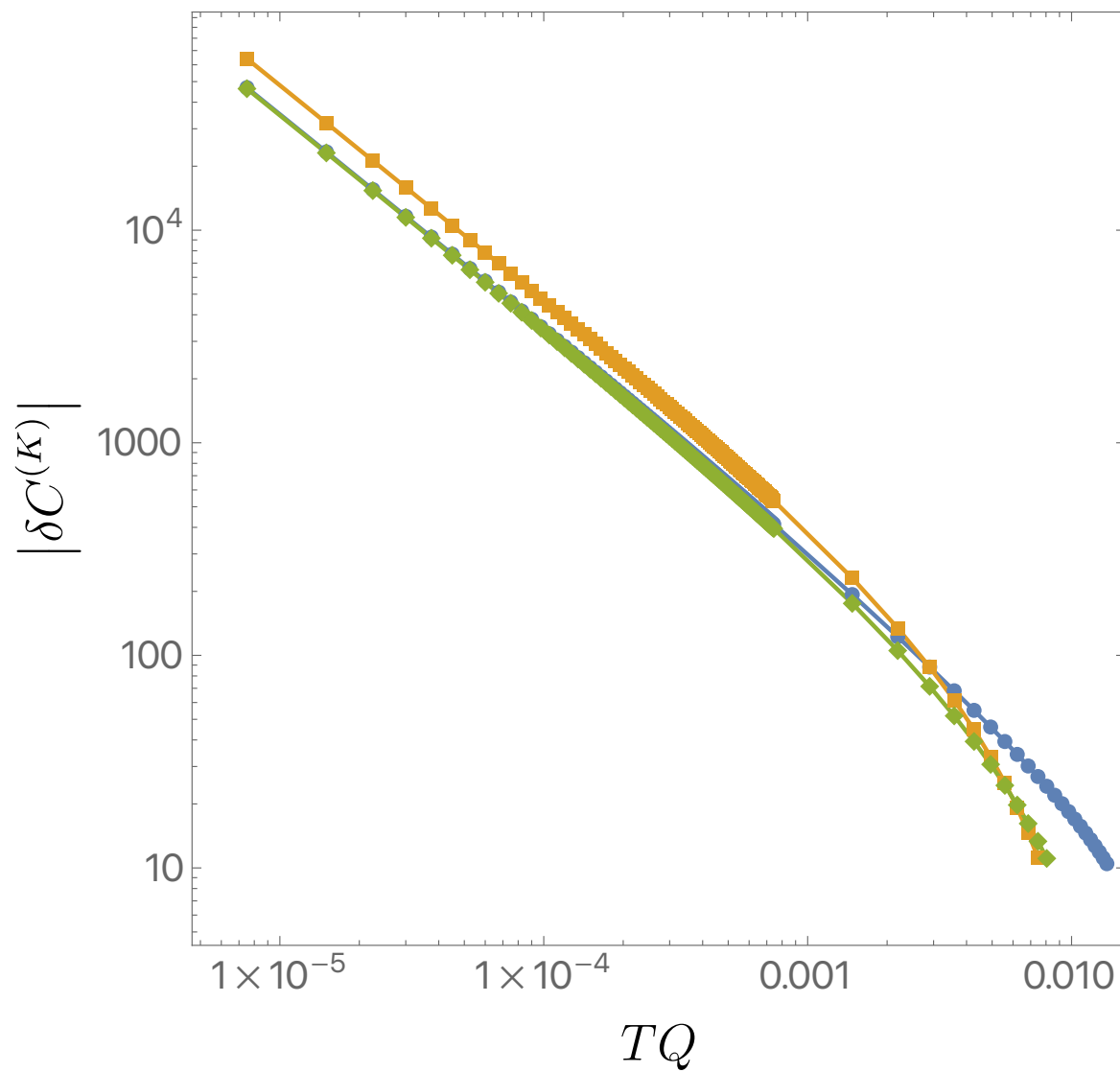
- Measure on horizon at equator: $C_{\varphi\varphi}^{\mathcal{H}}$
- Compare to un-corrected Kerr-Newman black hole with same charge, temperature, and angular momentum:

$$\delta C^{(K)} = \frac{Q^2}{d_K} \frac{C_{\varphi\varphi}^{\mathcal{H}} - \bar{C}_{\varphi\varphi}^{\mathcal{H}}}{\bar{C}_{\varphi\varphi}^{\mathcal{H}}}$$

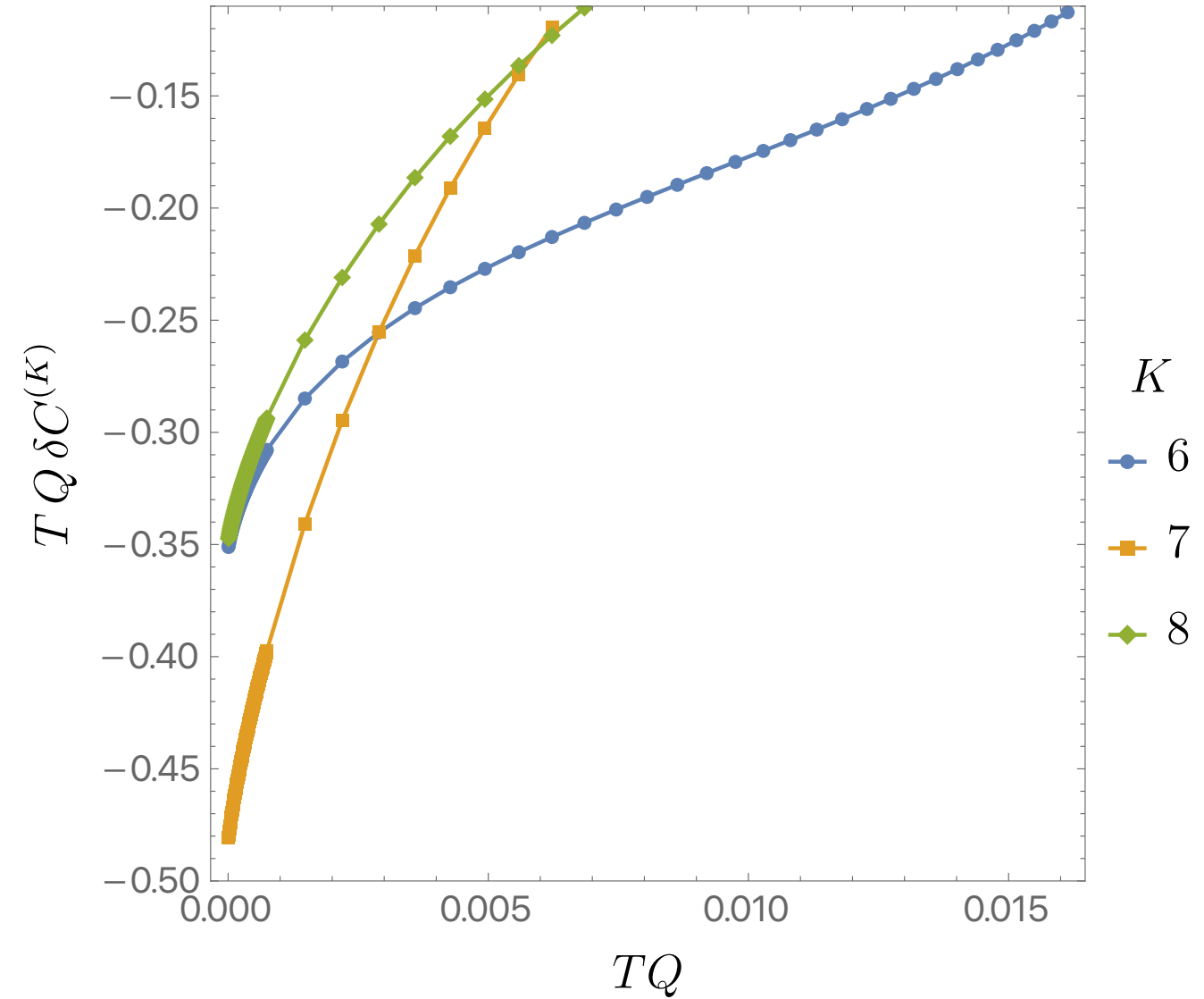


Probing the horizon singularity

$$\delta C^{(K)} = \frac{Q^2}{d_K} \frac{C_{\varphi\varphi}^{\mathcal{H}} - \bar{C}_{\varphi\varphi}^{\mathcal{H}}}{\bar{C}_{\varphi\varphi}^{\mathcal{H}}}$$



At low temperatures, we see that
 $\delta C^{(K)} \propto 1/T$



Defining parameters $\alpha = \bar{a}/r_+$, $q = \bar{Q}/r_+$
Numerics plotted for $\alpha = q$

Thermodynamics

- Let us examine the thermodynamic properties of our solutions.
- Chemical potential and angular velocity defined as before.
- Parameters α and q define moduli space of solutions.
- Perturbations to Komar charges,

$$E = \bar{E} - \frac{4\pi}{\kappa^2 r_+} \sum_{K=1}^8 \alpha_0^K d_K$$

$$J = \bar{J} + \frac{4\pi}{\kappa^2} \sum_{K=1}^8 [\omega_0^K (1 + \alpha^2 + q^2) - 2\alpha \alpha_0^K] d_K$$

$$Q_e = \frac{4\pi\sqrt{2}}{\kappa^2} \left[\bar{Q} + \frac{1}{r_+} \sum_{K=1}^8 \rho_0^K d_K \right]$$

Thermodynamics

- Temperature: $T = \frac{1 - \mathfrak{a}^2 - \mathfrak{q}^2}{4\pi r_+(1 + \mathfrak{a}^2)} \left(1 + \frac{1}{2} \sum_{K=6}^8 [f_1^{(K)}(X, 0) - f_2^{(K)}(X, 0)] \frac{d_K}{r_+^2} \right)$
- Wald entropy for our explicit numerical solutions:

$$S = \frac{8\pi^2}{\kappa^2} (1 + \mathfrak{a}^2) r_+^2 \left\{ 1 + \frac{1}{4r_+^2} \sum_{K=6}^8 \int_{-1}^1 dX \left[f_2^{(K)}(X, 0) + f_3^{(K)}(X, 0) \right] d_K \right.$$
$$\left. - \frac{2\mathfrak{q}^2}{3r_+^2} \left[\frac{9 + 4\mathfrak{a}^2 + 3\mathfrak{a}^4}{(1 + \mathfrak{a}^2)^3} + \frac{3 \arctan \mathfrak{a}}{\mathfrak{a}} \right] d_6 \right\}$$

Thermodynamics

- Temperature: $T = \frac{1 - \mathfrak{a}^2 - \mathfrak{q}^2}{4\pi r_+(1 + \mathfrak{a}^2)} \left(1 + \frac{1}{2} \sum_{K=6}^8 [f_1^{(K)}(X, 0) - f_2^{(K)}(X, 0)] \frac{d_K}{r_+^2} \right)$
- Wald entropy for our explicit numerical solutions:

$$S = \frac{8\pi^2}{\kappa^2} (1 + \mathfrak{a}^2) r_+^2 \left\{ 1 + \frac{1}{4r_+^2} \sum_{K=6}^8 \int_{-1}^1 dX \left[f_2^{(K)}(X, 0) + f_3^{(K)}(X, 0) \right] d_K \right.$$

$$\left. - \frac{2\mathfrak{q}^2}{3r_+^2} \left[\frac{9 + 4\mathfrak{a}^2 + 3\mathfrak{a}^4}{(1 + \mathfrak{a}^2)^3} + \frac{3 \arctan \mathfrak{a}}{\mathfrak{a}} \right] d_6 \right\}$$

- Prediction using on-shell action (comparing black holes with same Komar charges):

Cheung, Liu, GR [1903.09156]

$$\Delta S = \beta \int d^3x \sqrt{-g} \Delta \mathcal{L}$$

Thermodynamics

- Temperature: $T = \frac{1 - \mathfrak{a}^2 - \mathfrak{q}^2}{4\pi r_+(1 + \mathfrak{a}^2)} \left(1 + \frac{1}{2} \sum_{K=6}^8 [f_1^{(K)}(X, 0) - f_2^{(K)}(X, 0)] \frac{d_K}{r_+^2} \right)$
- Wald entropy for our explicit numerical solutions:

$$S = \frac{8\pi^2}{\kappa^2} (1 + \mathfrak{a}^2) r_+^2 \left\{ 1 + \frac{1}{4r_+^2} \sum_{K=6}^8 \int_{-1}^1 dX \left[f_2^{(K)}(X, 0) + f_3^{(K)}(X, 0) \right] d_K \right.$$

$$\left. - \frac{2\mathfrak{q}^2}{3r_+^2} \left[\frac{9 + 4\mathfrak{a}^2 + 3\mathfrak{a}^4}{(1 + \mathfrak{a}^2)^3} + \frac{3 \arctan \mathfrak{a}}{\mathfrak{a}} \right] d_6 \right\}$$

- Prediction using on-shell action (comparing black holes with same Komar charges):

$$\Delta S(\mathfrak{a}, \mathfrak{q}) = \frac{16\pi^2(\mathfrak{a}^2 - 3)(3\mathfrak{a}^2 - 1)[1 - \xi - \mathfrak{a}^2(1 + \xi)]^2}{15\kappa^2\xi(1 + \xi)(1 + \mathfrak{a}^2)^4} (d_0 + d_6 - d_9)$$

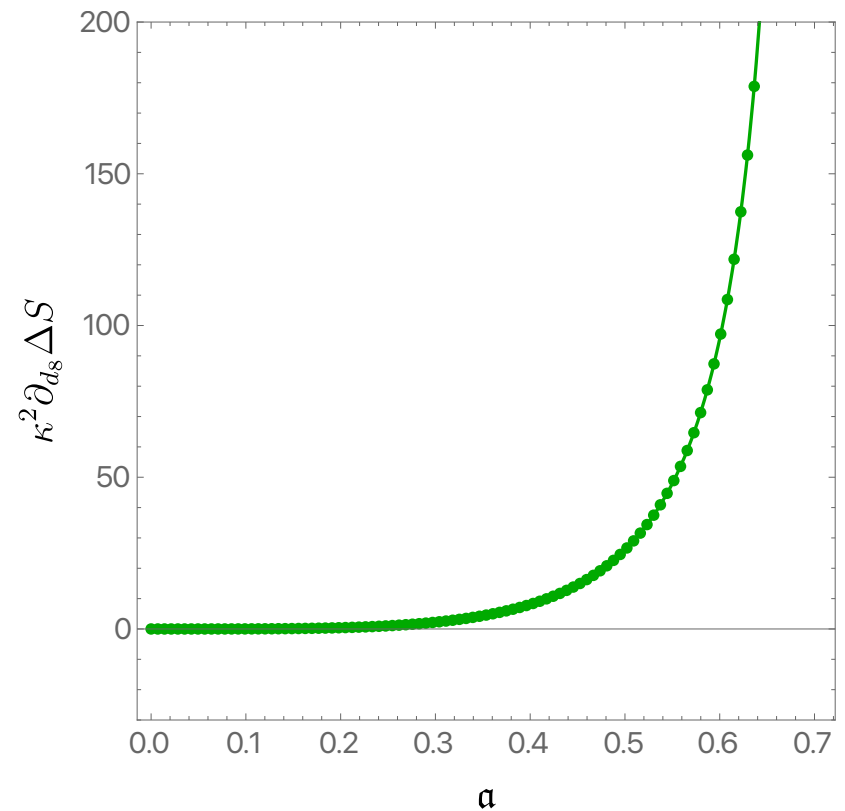
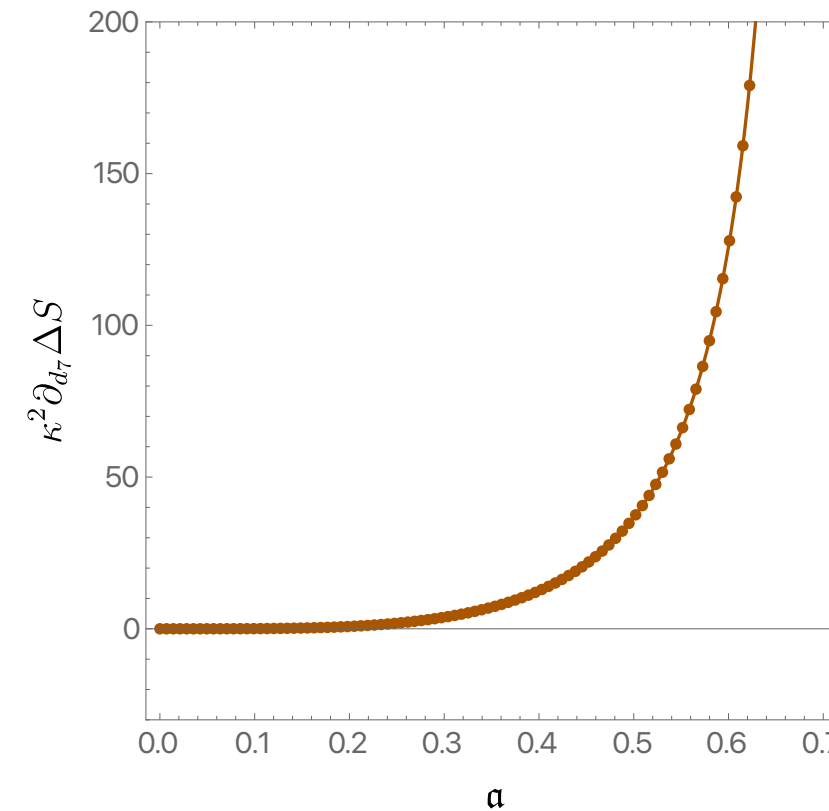
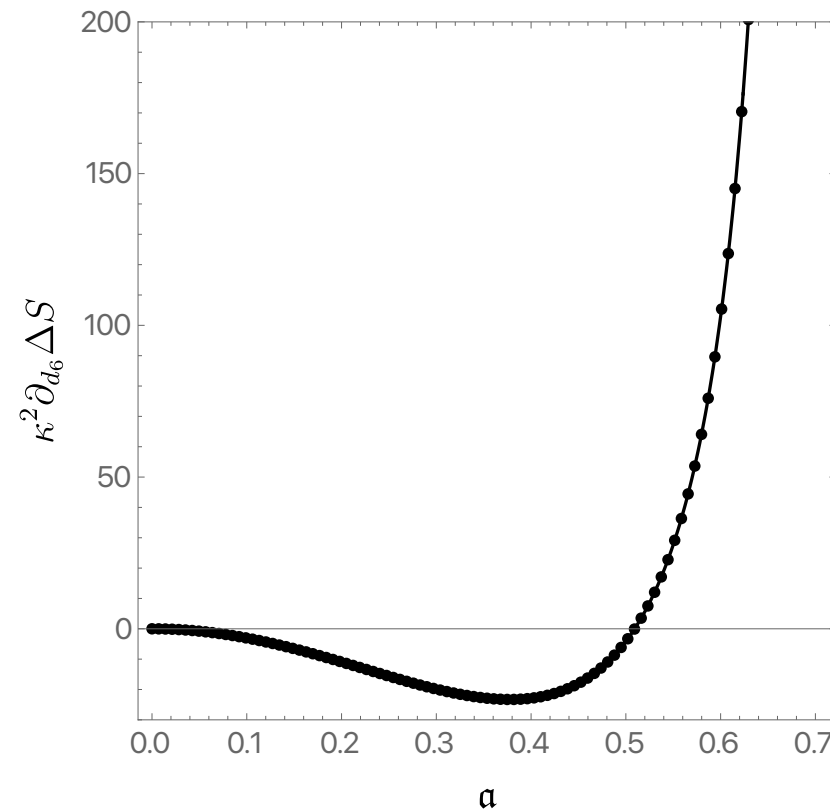
$$+ \frac{\pi^2 [1 - \xi - \mathfrak{a}^2(1 + \xi)]^2 [\mathfrak{a}(3 + 2\mathfrak{a}^2 + 3\mathfrak{a}^4) + 3(\mathfrak{a}^2 - 1)(1 + \mathfrak{a}^2)^2 \arctan \mathfrak{a}]}{2\kappa^2\xi(1 + \xi)\mathfrak{a}^5} (d_0 + d_6 + d_9)$$

$$+ \frac{64\pi^2}{\kappa^2} d_3 + \frac{32\pi^2[1 - \xi - \mathfrak{a}^2(1 + \xi)][\mathfrak{a}^2(3 + 4\xi) - 1 - 4\xi]}{5\kappa^2\xi(1 + \xi)(1 + \mathfrak{a}^2)^2} d_6$$

$$\xi = \frac{\sqrt{\bar{M}^2 - \bar{a}^2 - \bar{Q}^2}}{\bar{M}} = \frac{1 - \mathfrak{a}^2 - \mathfrak{q}^2}{1 + \mathfrak{a}^2 + \mathfrak{q}^2} = \frac{\kappa^2}{4\pi\bar{M}} \bar{T} \bar{S}$$

Thermodynamics

Numerical results for entropy precisely match our on-shell action prediction from euclidean quantum gravity:



Numerics plotted for $\alpha = q$

Back to extremal

- We can also use numerical methods to compute the full asymptotically flat metric for the EFT-corrected extremal black hole, and compare to our near-horizon analytical results.
- We use a slightly different compact coordinate, $r = r_+/(1 - Y^2)$

Back to extremal

- We can also use numerical methods to compute the full asymptotically flat metric for the EFT-corrected extremal black hole, and compare to our near-horizon analytical results.
- We use a slightly different compact coordinate, $r = r_+/(1 - Y^2)$

$$\begin{aligned} ds^2 = & - \frac{\Delta(r)}{\Sigma(r, X)} F_1(r, X) [dt - (1 - X^2) F_4(r, X) d\phi]^2 \\ & + \frac{1 - X^2}{\Sigma(r, X)} F_3(r, X) \Xi(r) [F_4(r, X) dt - (r^2 + \bar{a}^2) d\phi]^2 \\ & + \Sigma(r, X) F_2(r, X) \left[\frac{dr^2}{\Delta(r)} + \Xi(r) \frac{dX^2}{1 - X^2} \right] \end{aligned}$$

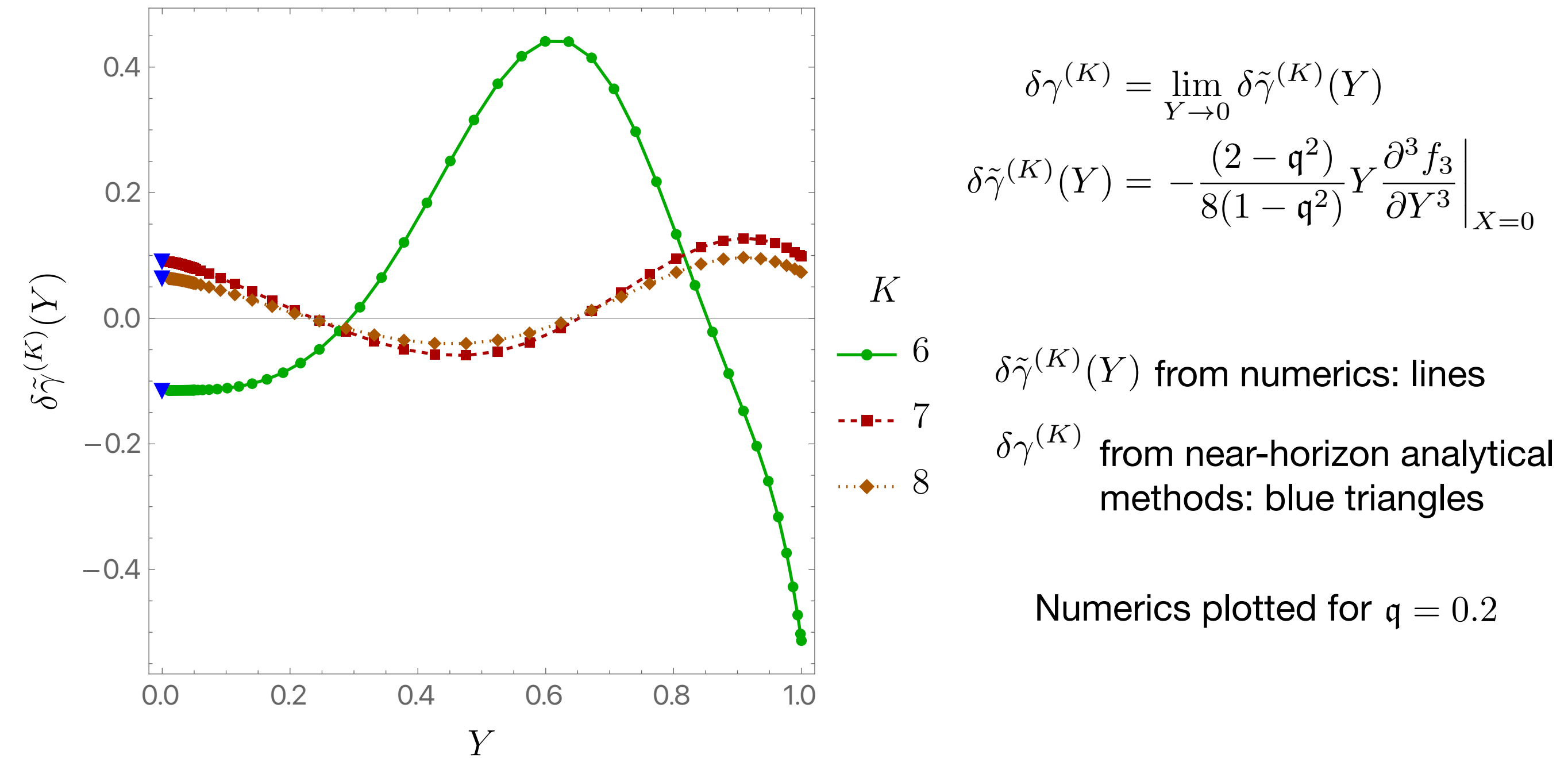
$$\Xi(r) = 1 + \sum_{K=6}^8 \frac{r_+^4}{r^4} \frac{d_K}{M^2} a^{(K)}$$

$$F_i(r, X) = 1 + \sum_{K=6}^8 \frac{d_K}{M^2} f_i^{(K)}(r, X), \quad i = 1, 2, 3 \quad F_5(r, X) = \bar{Q} + \left(1 - \frac{r_+}{r}\right) \sum_{K=6}^8 \frac{d_K}{M^2} f_5^{(K)}(r, X)$$

$$F_4(r, X) = \bar{a} + \left(1 - \frac{r_+}{r}\right) \sum_{K=6}^8 \frac{d_K}{M^2} f_4^{(K)}(r, X) \quad F_6(r, X) = \sum_{K=6}^8 \frac{d_K}{M^2} f_6^{(K)}(r, X)$$

Back to extremal

We can read off the shift in the scaling dimension for our mode of interest in terms of our numerical solution:



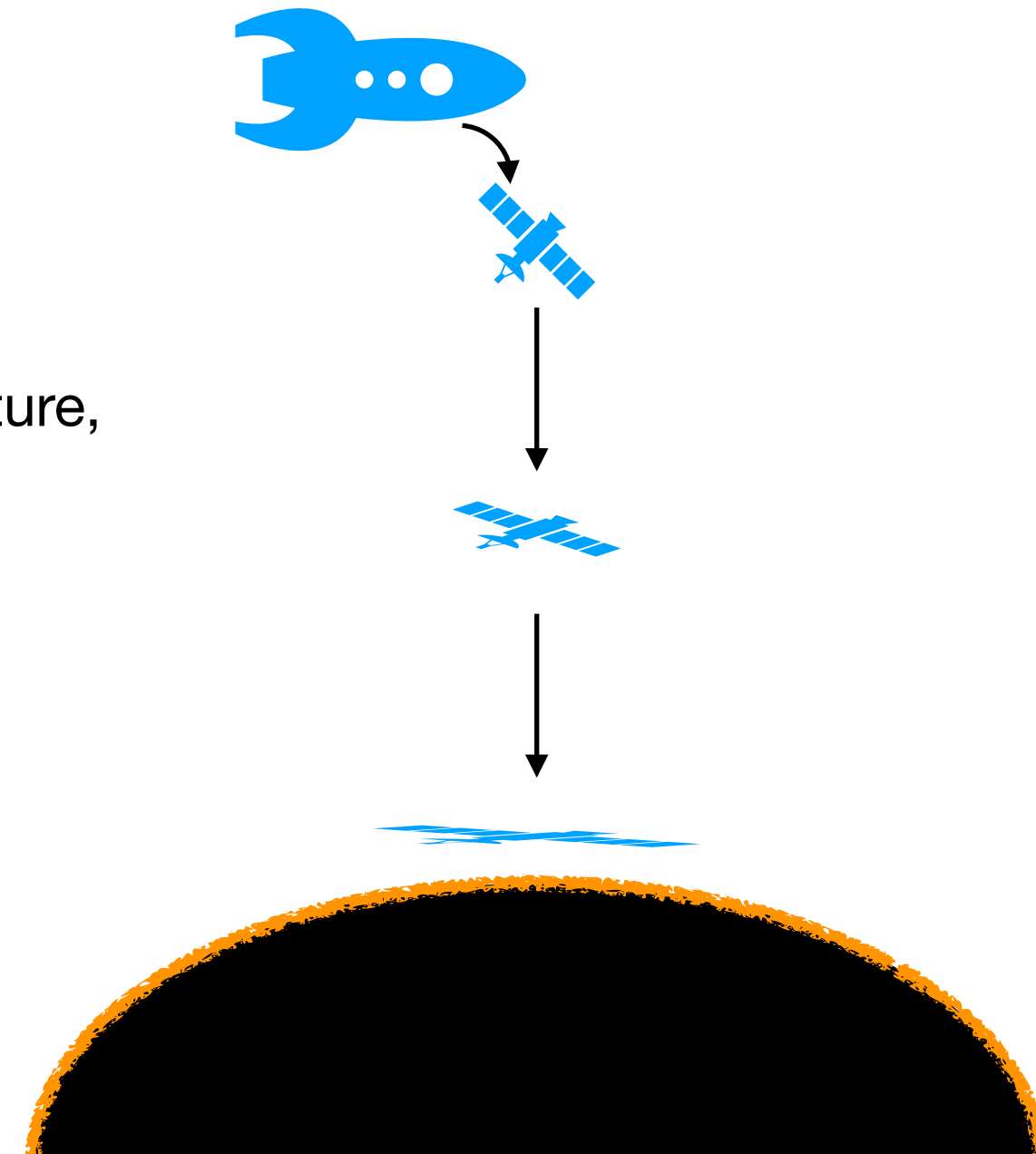
Probing the horizon singularity

- We can again construct a null geodesics heading towards the horizon and measure the tidal force.
- As before, define a tidal force observable:

$$C_{\varphi\varphi} = \dot{x}^a \dot{x}^b C_{\varphi a \varphi b}$$

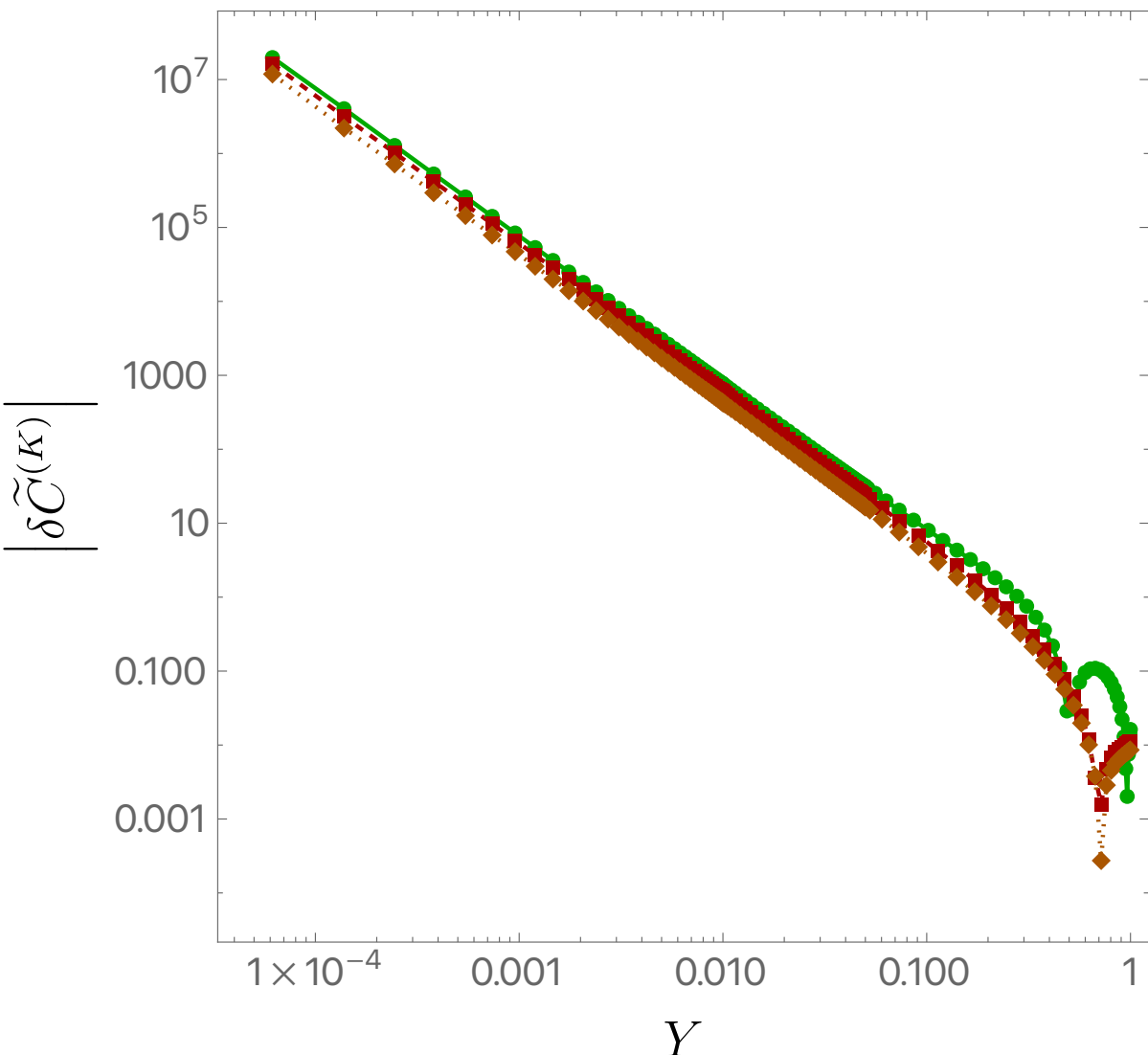
- Measure at equator, but do not restrict to horizon.
- Compare to un-corrected Kerr-Newman black hole with same charge, (zero) temperature, and angular momentum:

$$\delta \tilde{C}^{(K)} = \frac{\kappa^2 J}{8\pi d_K} \frac{C_{\varphi\varphi}^{X=0} - \bar{C}_{\varphi\varphi}^{X=0}}{\bar{C}_{\varphi\varphi}^{X=0}}$$

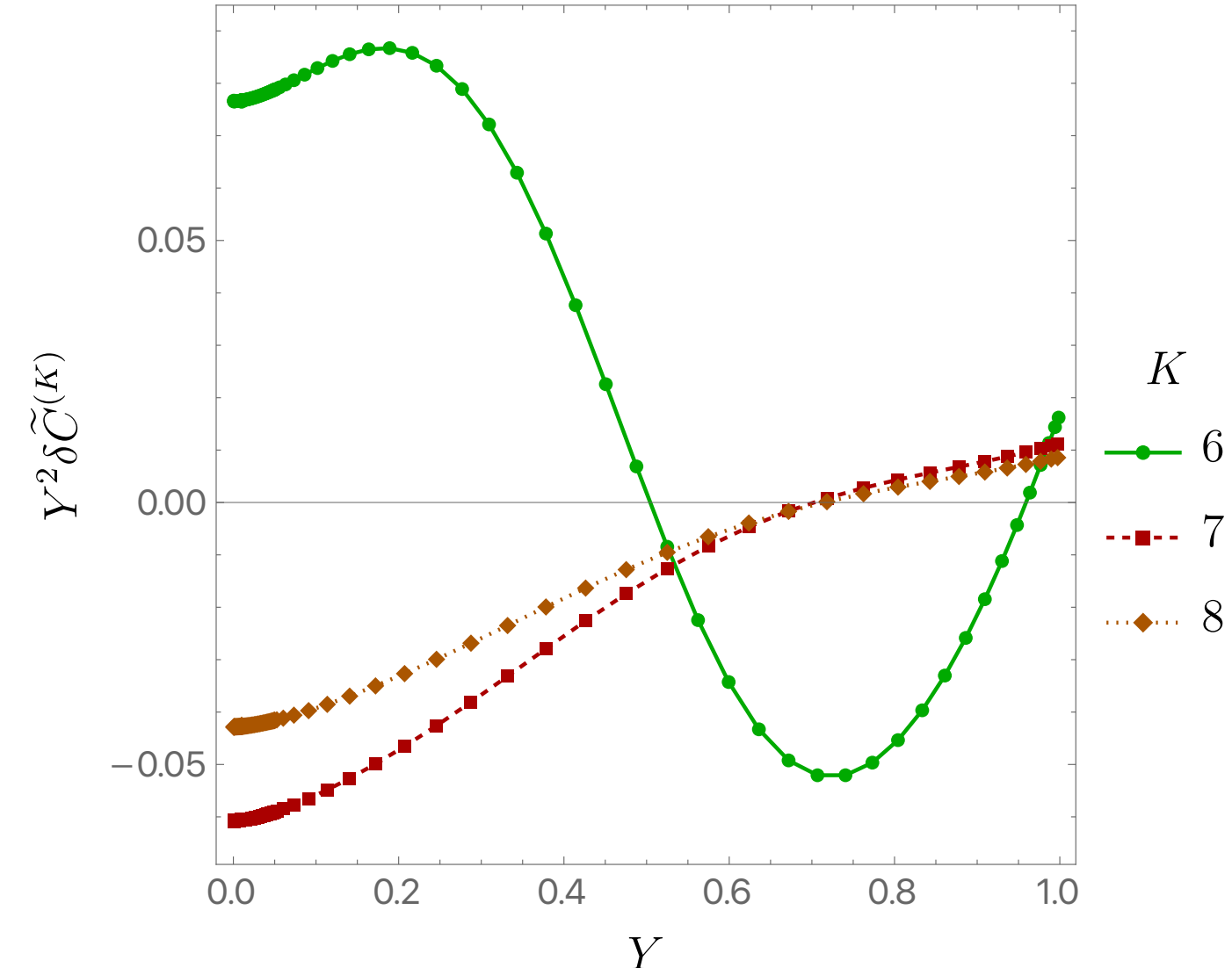


Probing the horizon singularity

$$\delta \tilde{C}^{(K)} = \frac{\kappa^2 J}{8\pi d_K} \frac{C_{\varphi\varphi}^{X=0} - \bar{C}_{\varphi\varphi}^{X=0}}{\bar{C}_{\varphi\varphi}^{X=0}}$$



Close to the horizon, we see that
 $\delta \tilde{C}^{(K)} \propto 1/Y^2 \sim 1/(r - r_+)$

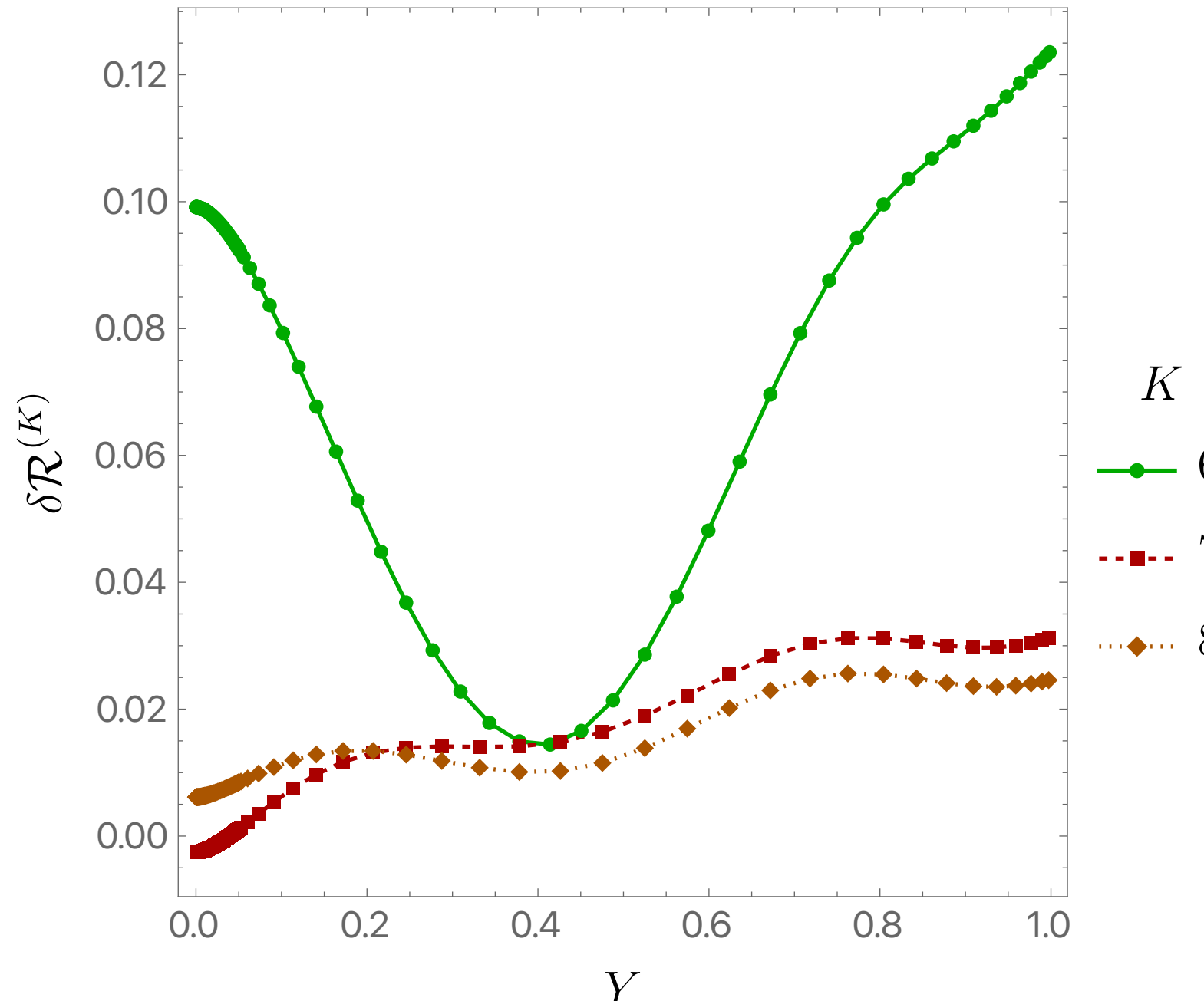


Numerics plotted for $q = 0.2$

Probing the horizon singularity

- Interestingly, all curvature *invariants* remain finite on the horizon.
- Correction to KN metric $\delta g \sim \rho^\gamma$
 \implies curvature $\delta C \sim \rho^{\gamma-2}$
- Equations of motion are second-rank tensor, and all but two ρ derivatives in any invariant are contracted with $g^{\rho\rho} = \rho^2$
 \implies no higher divergence
- Example:

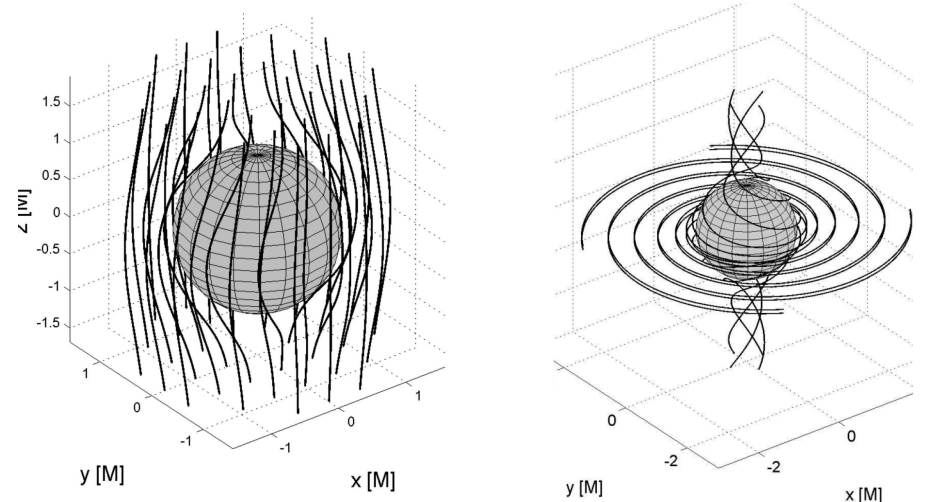
$$\delta\mathcal{R}^{(K)} = \frac{\kappa^2 J}{8\pi d_K} \left. \frac{R_{abcd}R^{abcd} - \bar{R}_{abcd}\bar{R}^{abcd}}{\bar{R}_{abcd}\bar{R}^{abcd}} \right|_{X=0}$$



Astrophysics

Charge on astrophysical black holes?

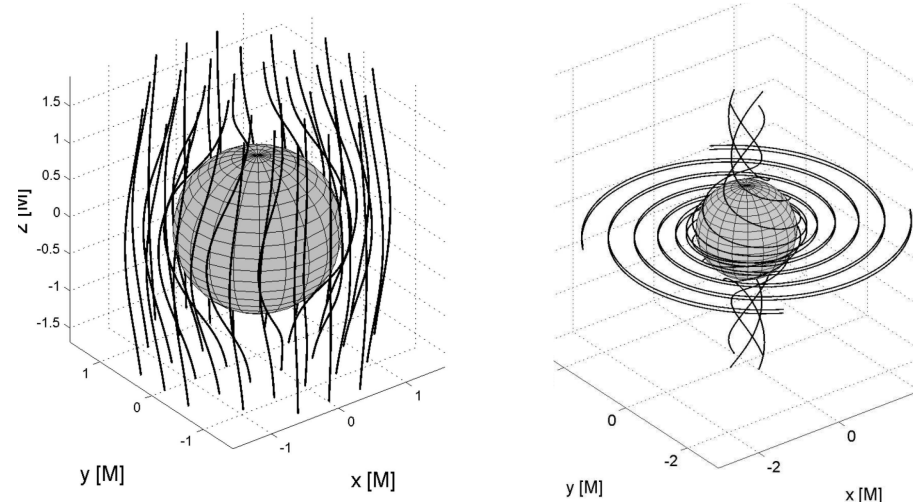
- Black hole in plasma: $Q/M \sim m_e/q_e \sim 10^{-21}$
- Wald effect: a black hole spinning in a magnetic field produces an electric field on the horizon, leading to accumulation of equilibrium charge $Q_W = 2BaM$ [Wald \(1974\)](#)



[Karas, Kopáček, Kunneriath \[1201.0009\]](#)

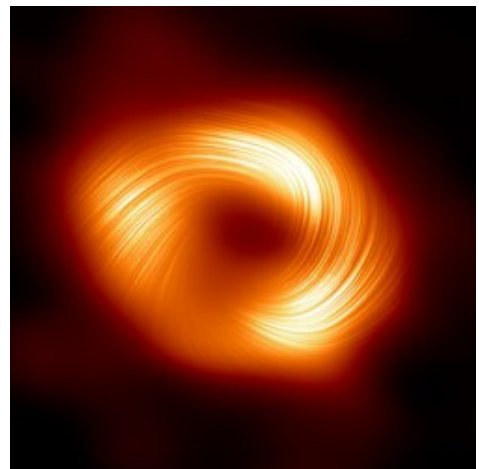
Charge on astrophysical black holes?

- Black hole in plasma: $Q/M \sim m_e/q_e \sim 10^{-21}$
- Wald effect: a black hole spinning in a magnetic field produces an electric field on the horizon, leading to accumulation of equilibrium charge $Q_W = 2BaM$ [Wald \(1974\)](#)



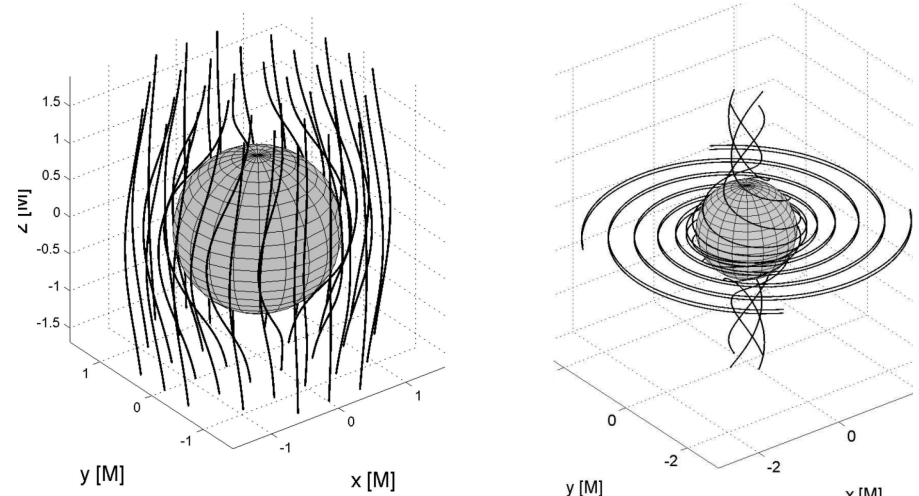
[Karas, Kopáček, Kunneriath \[1201.0009\]](#)

- For Sag A*, the galactic magnetic field of 10 G induces a charge-to-mass ratio of $Q/M \sim 10^{-12}$ [Zajaček, Tursunov \[1904.04654\]](#)



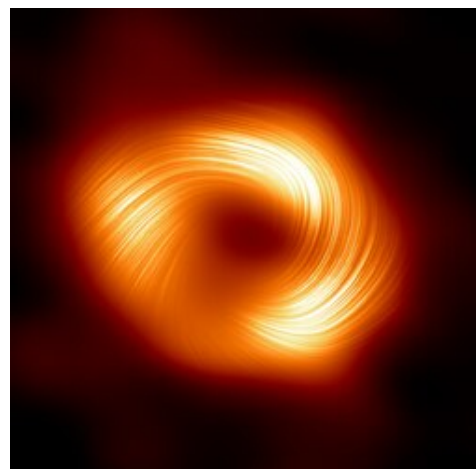
Charge on astrophysical black holes?

- Black hole in plasma: $Q/M \sim m_e/q_e \sim 10^{-21}$
- Wald effect: a black hole spinning in a magnetic field produces an electric field on the horizon, leading to accumulation of equilibrium charge $Q_W = 2BaM$ [Wald \(1974\)](#)



[Karas, Kopáček, Kunneriath \[1201.0009\]](#)

- For Sag A*, the galactic magnetic field of 10 G induces a charge-to-mass ratio of $Q/M \sim 10^{-12}$ [Zajaček, Tursunov \[1904.04654\]](#)



- Black hole collision with a typical pulsar (10 M_\odot black hole, 10 km apart, 10¹² G), $Q/M \sim 10^{-7}$ [Levin, D'Orazio, Garcia-Saenz \[1808.07887\]](#)



Rough estimate

- Shift in scaling dimension $\delta\gamma \sim Gc_{7,8}F^4(GM)^2 \sim c_{7,8}Z^4/G^3M^2$
- Standard model contribution to Euler-Heisenberg Lagrangian $c_{7,8} \sim 10^{-4}(q_e/m_e)^4$
$$\implies \delta\gamma \sim 10^{81}Z^4/S$$
$$\implies C_{\rho\phi\rho\phi}|_H \sim 10^{81} \frac{Z^4}{GMST}$$

Rough estimate

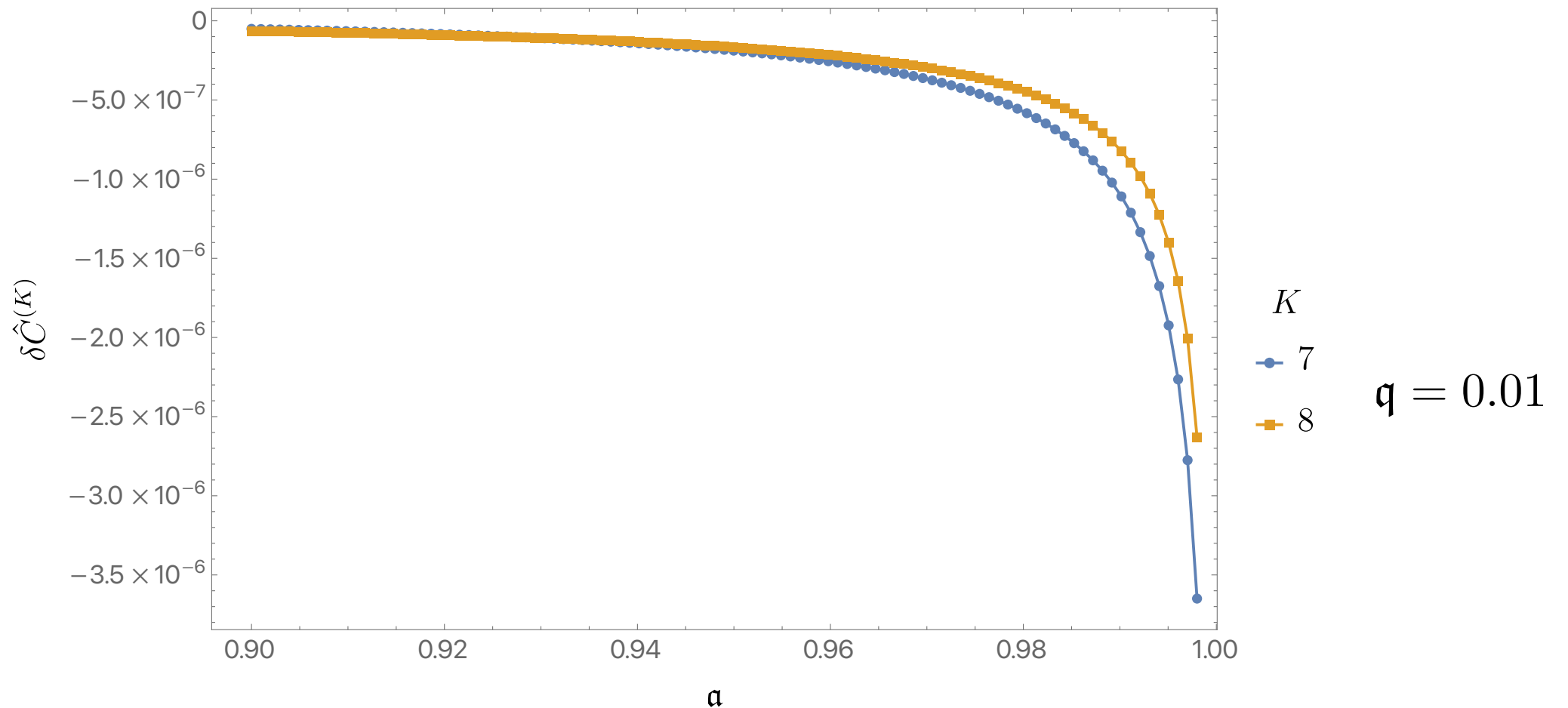
- Shift in scaling dimension $\delta\gamma \sim Gc_{7,8}F^4(GM)^2 \sim c_{7,8}Z^4/G^3M^2$
- Standard model contribution to Euler-Heisenberg Lagrangian $c_{7,8} \sim 10^{-4}(q_e/m_e)^4$
$$\implies \delta\gamma \sim 10^{81}Z^4/S$$
$$\implies C_{\rho\phi\rho\phi}|_H \sim 10^{81} \frac{Z^4}{GMST}$$
- Quantum corrections? $T_q = \frac{\pi}{GMS} \ll T_{\text{EFT}} \sim \frac{10^{81}Z^4}{GMS}$
[Rajiv, Rangamani, Turiaci \[2310.04532\]](#);
[Kapec, Sheta, Strominger, Toldo \[2310.00848\]](#)

Rough estimate

- Shift in scaling dimension $\delta\gamma \sim Gc_{7,8}F^4(GM)^2 \sim c_{7,8}Z^4/G^3M^2$
- Standard model contribution to Euler-Heisenberg Lagrangian $c_{7,8} \sim 10^{-4}(q_e/m_e)^4$
$$\implies \delta\gamma \sim 10^{81}Z^4/S$$
$$\implies C_{\rho\phi\rho\phi}|_H \sim 10^{81} \frac{Z^4}{GMST}$$
- Quantum corrections? $T_q = \frac{\pi}{GMS} \ll T_{\text{EFT}} \sim \frac{10^{81}Z^4}{GMS}$
[Rajiv, Rangamani, Turiaci \[2310.04532\]](#);
[Kapec, Sheta, Strominger, Toldo \[2310.00848\]](#)
- For a typical black hole colliding with a neutron star, $T_{\text{EFT}} \sim 10^{-25}/GM$, so this effect is too small to be observable in that case.
- Exotic scenarios and probes of the dark sector: new light particles or forces, e.g., $U(1)_{B-L}$ charges, are a direction of future interest.

Numerical results for astrophysics

- Let us use our numerical results to assess the best-case astrophysical scenario for observation of our EFT enhancement effect.
- Maximum realistic astrophysical spin: $a \approx 0.998$ [Thorne \(1974\)](#)
(spin-up from hot accretion disk balanced by torque from thermal radiation)
- Numerical results: $\delta\hat{C}^{(K)} = \frac{\kappa^2 J}{8\pi d_K} \frac{C_{\varphi\varphi}^{\mathcal{H}} - \bar{C}_{\varphi\varphi}^{\mathcal{H}}}{\bar{C}_{\varphi\varphi}^{\mathcal{H}}} \sim (5 \text{ to } 300) \times q^4$



Numerical results for astrophysics

- Let us use our numerical results to assess the best-case astrophysical scenario for observation of our EFT enhancement effect.
- Maximum realistic astrophysical spin: $a \approx 0.998$ [Thorne \(1974\)](#)
(spin-up from hot accretion disk balanced by torque from thermal radiation)
- Using standard model values of the Wilson coefficients,

$$\frac{C_{\varphi\varphi}^{\mathcal{H}} - \bar{C}_{\varphi\varphi}^{\mathcal{H}}}{\bar{C}_{\varphi\varphi}^{\mathcal{H}}} \sim (10^5 \text{ to } 10^7) \times \left(\frac{10 M_{\odot}}{M} \right)^2 \times q^4$$

Numerical results for astrophysics

- Let us use our numerical results to assess the best-case astrophysical scenario for observation of our EFT enhancement effect.
- Maximum realistic astrophysical spin: $a \approx 0.998$ [Thorne \(1974\)](#)
(spin-up from hot accretion disk balanced by torque from thermal radiation)
- Using standard model values of the Wilson coefficients,

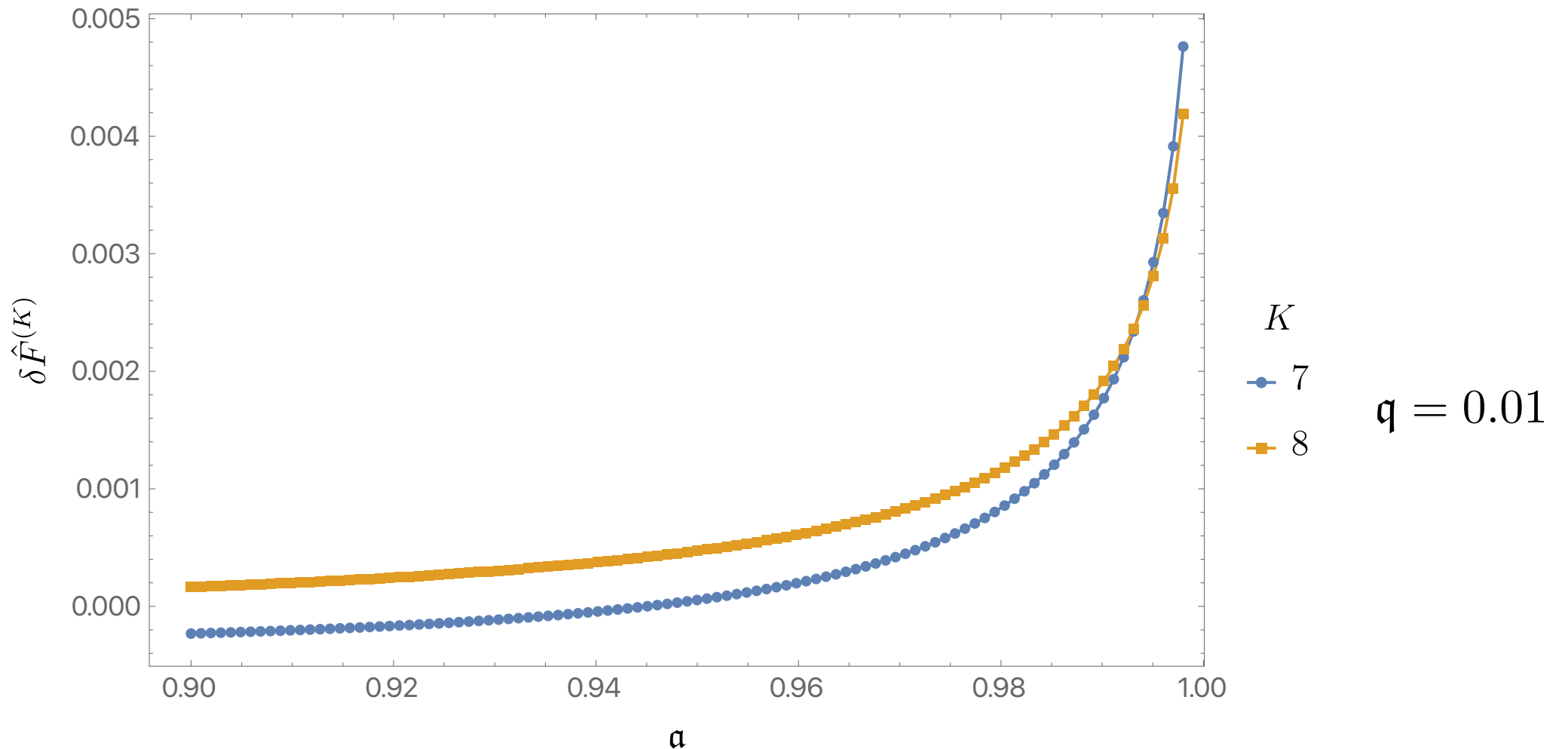
$$\frac{C_{\varphi\varphi}^{\mathcal{H}} - \bar{C}_{\varphi\varphi}^{\mathcal{H}}}{\bar{C}_{\varphi\varphi}^{\mathcal{H}}} \sim (10^5 \text{ to } 10^7) \times \left(\frac{10 M_{\odot}}{M} \right)^2 \times q^4$$

- Induced Wald charge largest for black hole of same size as neutron star, $M = 7 M_{\odot}$
$$\frac{C_{\varphi\varphi}^{\mathcal{H}} - \bar{C}_{\varphi\varphi}^{\mathcal{H}}}{\bar{C}_{\varphi\varphi}^{\mathcal{H}}} \sim (10^{-8} \text{ to } 10^{-6}) \times (B/10^{16} \text{ G})^4$$
- Strongest magnetars have fields up to 10^{16} G [Raynaud et al. \[2003.06662\]](#) $\implies q \sim 2 \times 10^{-4}$
- Observable with future precision GW measurements?

Numerical results for astrophysics

- What about electrodynamic observables? Numerical analysis gives

$$\delta \hat{\mathcal{F}}^{(K)} = \frac{\kappa^2 J}{8\pi d_K} \frac{\mathcal{F} - \bar{\mathcal{F}}}{\bar{\mathcal{F}}} \sim (2 \text{ to } 50) \times q^2 \text{ for } \mathcal{F} = \dot{x}^a F_{a\varphi}$$



- Best-case astrophysical scenario:

$$\frac{\mathcal{F} - \bar{\mathcal{F}}}{\bar{\mathcal{F}}} \gtrsim \text{few percent}$$

Naive EFT estimate:

$$\delta \mathcal{F}^{(K)} \sim 16q^2$$

Discussion

EFT breaking?

- The derivative expansion of the bulk Lagrangian remains under control: yet-higher derivative Lorentz scalars do not diverge, and with smaller Wilson coefficients contribute negligibly to the action.
 \Rightarrow Calculations of the EFT-corrected background geometry remain robust.

EFT breaking?

- The derivative expansion of the bulk Lagrangian remains under control: yet-higher derivative Lorentz scalars do not diverge, and with smaller Wilson coefficients contribute negligibly to the action.
⇒ Calculations of the EFT-corrected background geometry remain robust.
- Different story for the worldline EFT of an observer: Contraction into velocity vector allows for divergence in $\dot{x}^a \dot{x}^b C_{a\varphi b\varphi}$
⇒ finite-size effects diverge, e.g., Love numbers associated with gravitoelectric tensor $E_{ab}^2 = (C_{acbd} \dot{x}^c \dot{x}^d)^2$ [Cheung, Solon \[2006.06665\]](#)

EFT breaking?

- The derivative expansion of the bulk Lagrangian remains under control: yet-higher derivative Lorentz scalars do not diverge, and with smaller Wilson coefficients contribute negligibly to the action.
 \Rightarrow Calculations of the EFT-corrected background geometry remain robust.
- Different story for the worldline EFT of an observer: Contraction into velocity vector allows for divergence in $\dot{x}^a \dot{x}^b C_{a\varphi b\varphi}$
 \Rightarrow finite-size effects diverge, e.g., Love numbers associated with gravitoelectric tensor $E_{ab}^2 = (C_{acbd} \dot{x}^c \dot{x}^d)^2$ [Cheung, Solon \[2006.06665\]](#)
- Worldline EFT breaks down, leading to loss of predictability: experience of infalling observer is dictated by the UV. (Firewalls?)

EFT breaking?

- The derivative expansion of the bulk Lagrangian remains under control: yet-higher derivative Lorentz scalars do not diverge, and with smaller Wilson coefficients contribute negligibly to the action.
 \Rightarrow Calculations of the EFT-corrected background geometry remain robust.
- Different story for the worldline EFT of an observer: Contraction into velocity vector allows for divergence in $\dot{x}^a \dot{x}^b C_{a\varphi b\varphi}$
 \Rightarrow finite-size effects diverge, e.g., Love numbers associated with gravitoelectric tensor $E_{ab}^2 = (C_{acbd} \dot{x}^c \dot{x}^d)^2$ [Cheung, Solon \[2006.06665\]](#)
- Worldline EFT breaks down, leading to loss of predictability: experience of infalling observer is dictated by the UV. (Firewalls?)
- Infalling string: horizon looks like singular plane wave geometry, and a string can get highly excited if $\gamma \leq 1$

Future directions

- Adding large external magnetic field: Kerr-Newman black hole in a constant ambient magnetic field has exact solution. EFT-correct this spacetime to more precisely simulate astrophysical scenarios?

Future directions

- Adding large external magnetic field: Kerr-Newman black hole in a constant ambient magnetic field has exact solution. EFT-correct this spacetime to more precisely simulate astrophysical scenarios?
- Explore the phenomenology of non-standard model charges and/or light hidden sectors

Future directions

- Adding large external magnetic field: Kerr-Newman black hole in a constant ambient magnetic field has exact solution. EFT-correct this spacetime to more precisely simulate astrophysical scenarios?
- Explore the phenomenology of non-standard model charges and/or light hidden sectors
- Dynamical stability: does horizon singularity indicate instability? If so, what is the endpoint? Superradiance?

Future directions

- Adding large external magnetic field: Kerr-Newman black hole in a constant ambient magnetic field has exact solution. EFT-correct this spacetime to more precisely simulate astrophysical scenarios?
- Explore the phenomenology of non-standard model charges and/or light hidden sectors
- Dynamical stability: does horizon singularity indicate instability? If so, what is the endpoint? Superradiance?
- EFT corrections to black holes in AdS, in supersymmetric theories, or string theory (EFT-corrected GHS?)

Questions